N-1833

June 1991

NCEL

Technical Note

By L. J. Malvar

Sponsored By Office of
Naval Research

# BOND OF REINFORCEMENT UNDER CONTROLLED CONFINEMENT





**ABSTRACT** Twelve specimens were tested to determine the local bond stress-slip characteristics of a No. 6 rebar embedded in a 3-inch diameter concrete cylinder. Radial confining stress around the concrete specimen and radial deformation were assumed to be fundamental variables, together with bond stress and slip, needed to properly describe the interface behavior. Configuration independent bond stress-slip relationships for a short five-lug embedded length were obtained for various degrees of confining pressure. Maximum bond stresses could be increased almost threefold by increasing the confining stress from 500 to 4500 psi at the bar level. Two types of No. 6 bars with different deformations were investigated.

NAVAL CIVIL ENGINEERING LABORATORY PORT HUENEME CALIFORNIA 93043-5003

## METRIC CONVERSION FACTORS

### Approximate Conversions to Metric Measures

| Symbol | When You Know | Multiply by | To Find | Symbol |
|---|---|---|---|---|
| | | **LENGTH** | | |
| in | inches | *2.5 | centimeters | cm |
| ft | feet | 30 | centimeters | cm |
| yd | yards | 0.9 | meters | m |
| mi | miles | 1.6 | kilometers | km |
| | | **AREA** | | |
| $in^2$ | square inches | 6.5 | square centimeters | $cm^2$ |
| $ft^2$ | square feet | 0.09 | square meters | $m^2$ |
| $yd^2$ | square yards | 0.8 | square meters | $m^2$ |
| $mi^2$ | square miles | 2.6 | square kilometers | $km^2$ |
| | acres | 0.4 | hectares | ha |
| | | **MASS (weight)** | | |
| oz | ounces | 28 | grams | g |
| lb | pounds | 0.45 | kilograms | kg |
| | short tons (2,000 lb) | 0.9 | tonnes | t |
| | | **VOLUME** | | |
| tsp | teaspoons | 5 | milliliters | ml |
| Tbsp | tablespoons | 15 | milliliters | ml |
| fl oz | fluid ounces | 30 | milliliters | ml |
| c | cups | 0.24 | liters | l |
| pt | pints | 0.47 | liters | l |
| qt | quarts | 0.95 | liters | l |
| gal | gallons | 3.8 | liters | l |
| $ft^3$ | cubic feet | 0.03 | cubic meters | $m^3$ |
| $yd^3$ | cubic yards | 0.76 | cubic meters | $m^3$ |
| | | **TEMPERATURE (exact)** | | |
| °F | Fahrenheit temperature | 5/9 (after subtracting 32) | Celsius temperature | °C |

*1 in = 2.54 (exactly). For other exact conversions and more detailed tables, see NBS Misc. Publ. 286, Units of Weights and Measures, Price $2.25, SD Catalog No. C13.10:286.


### Approximate Conversions from Metric Measures

| Symbol | When You Know | Multiply by | To Find | Symbol |
|---|---|---|---|---|
| | | **LENGTH** | | |
| mm | millimeters | 0.04 | inches | in |
| cm | centimeters | 0.4 | inches | in |
| m | meters | 3.3 | feet | ft |
| m | meters | 1.1 | yards | yd |
| km | kilometers | 0.6 | miles | mi |
| | | **AREA** | | |
| $cm^2$ | square centimeters | 0.16 | square inches | $in^2$ |
| $m^2$ | square meters | 1.2 | square yards | $yd^2$ |
| $km^2$ | square kilometers | 0.4 | square miles | $mi^2$ |
| ha | hectares (10,000 $m^2$) | 2.5 | acres | |
| | | **MASS (weight)** | | |
| g | grams | 0.035 | ounces | oz |
| kg | kilograms | 2.2 | pounds | lb |
| t | tonnes (1,000 kg) | 1.1 | short tons | |
| | | **VOLUME** | | |
| ml | milliliters | 0.03 | fluid ounces | fl oz |
| l | liters | 2.1 | pints | pt |
| l | liters | 1.06 | quarts | qt |
| l | liters | 0.26 | gallons | gal |
| $m^3$ | cubic meters | 35 | cubic feet | $ft^3$ |
| $m^3$ | cubic meters | 1.3 | cubic yards | $yd^3$ |
| | | **TEMPERATURE (exact)** | | |
| °C | Celsius temperature | 9/5 (then add 32) | Fahrenheit temperature | °F |

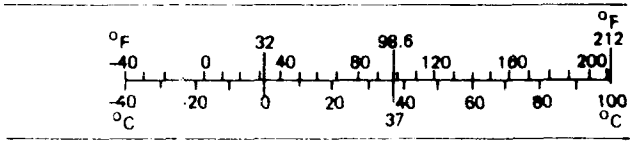

# REPORT DOCUMENTATION PAGE

*Form Approved*
*OMB No. 0704-018*



| 1. AGENCY USE ONLY *(Leave blank)* | 2. REPORT DATE | 3. REPORT TYPE AND DATES COVERED |
|---|---|---|
| | June 1991 | Final - Oct 1989 to Feb 1991 |

**4. TITLE AND SUBTITLE**

**BOND OF REINFORCEMENT UNDER CONTROLLED CONFINEMENT**

**5. FUNDING NUMBERS**

WU - DN666342
PR - YR023.03.001

**6. AUTHOR(S)**

L.J. Malvar, Assistant Research Engineer
University of California, Davis

**7. PERFORMING ORGANIZATION NAME(S) AND ADDRESSE(S)**

Naval Civil Engineering Laboratory
Port Hueneme, CA 93043-5003

**8. PERFORMING ORGANIZATION REPORT NUMBER**

**TN - 1833**

**9 SPONSORING/MONITORING AGENCY NAME(S) AND ADDRESSE(S)**

Office of Naval Research
Arlington, VA 22217-5000

**10. SPONSORING/MONITORING AGENCY REPORT NUMBER**

**11. SUPPLEMENTARY NOTES**

**12a. DISTRIBUTION/AVAILABILITY STATEMENT**

Approved for public release; distribution is unlimited.

**12b. DISTRIBUTION CODE**

**13. ABSTRACT** *(Maximum 200 words)*

Twelve specimens were tested to determine the local bond stress-slip characteristics of a No. 6 rebar embedded in a 3-inch diameter concrete cylinder. Radial confining stress around the concrete specimen and radial deformation were assumed to be fundamental variables, together with bond stress and slip, needed to properly describe the interface behavior. Configuration independent bond stress-slip, relationships for a short five-lug embedded length were obtained for various degrees of confining pressure. Maximum bond stresses could be increased almost threefold by increasing the confining stress from 500 to 4500 psi at the bar level. Two types of No. 6 bars with different deformations were investigated.

**14. SUBJECT TERMS**

Bond, concrete, reinforcement, steel, confinement

**15. NUMBER OF PAGES**

45

**16. PRICE CODE**

| 17. SECURITY CLASSIFICATION OF REPORT | 18. SECURITY CLASSIFICATION OF THIS PAGE | 19. SECURITY CLASSIFICATION OF ABSTRACT | 20. LIMITATION OF ABSTRACT |
|---|---|---|---|
| Unclassified | Unclassified | Unclassified | UL |

## CONTENTS

## INTRODUCTION

Twelve specimens were tested to determine the local bond stress-slip characteristics of a No. 6 rebar embedded in concrete. Radial confining stress around the concrete specimen and radial deformation were assumed to be fundamental variables, together with bond stress and slip, needed to properly describe the interface behavior.

The objectives of the research were to:

- Establish the necessity for considering radial stress and radial deformation in the study of bond phenomena.
- Show that observed bond characteristics are sensitive to test specimen configuration.
- Determine configuration independent local bond stress-slip relationships for two types of No. 6 bars with different deformations.

## RESEARCH SIGNIFICANCE

In many reinforced concrete structures, the mode of failure is tensile cracking of the concrete. Where it is important to predict failure or severe damage, proper representation of bond is crucial.

The principal gain from the inclusion of actual bond-slip properties in the interface between steel rebar and concrete is a realistic prediction of cracking. The spacing, width, and extent of cracks in reinforced concrete are all dependent on the assumed bond-slip characteristics (Ref 1). For example, if perfect bond is assumed in the finite element analysis of a cylindrical concrete specimen with one central bar in tension, the cracks will erroneously concentrate at the edges (Ref 1). On the other hand, perfect bond in a beam in four point bending will homogenize the strain field and diffuse the numerical crack pattern (Ref 2, 3, and 4). In turn, the crack pattern will impact the internal distribution of forces, the effective stiffness of the member, its ultimate strength and mode of failure (Ref 1). Shear failures, for example, often originate by propagation of existing bending cracks.

Critical Navy reinforced concrete structures, such as missile test cells and graving drydocks, are designed to withstand large deformations under severe blast and strong-motion earthquake loads. The development of design criteria for these structures requires the evaluation of their response in the nonlinear range where severe deterioration of the steel/concrete interface takes place. Accurate modeling of the nonlinear response requires a knowledge of the interface behavior for large deformations.

Extant studies on bond-slip typically ignore the effects of radial stress and deformation. The strong dependency of bond-slip on those two radial variables implies a dependency of previous test results on the particular specimen configuration used. The present test setup aims at providing general local relationships that would be applicable for any configuration.

## BOND MECHANISM

The mechanism of bond is comprised of three main components: chemical adhesion, friction, and mechanical interlock between bar ribs and concrete. Initially, for very small values of bond stress of up to 200 psi (Ref 5 and 6), chemical adhesion is the main resisting mechanism. If the bond stress is increased, chemical adhesion is destroyed and replaced by the wedging action of the ribs. This wedging action originates crushing in front of the ribs, secondary internal transverse (or radial) cracks (Figure 1) (Ref 7 and 8), and eventually longitudinal cracks. Early crushing of the concrete in front of the ribs explains the non-linearity of the ascending branch (Figure 2). Once enough crushing has occurred, a wedge of compacted powder forms in front of the rib, with a low angle of incidence (around 30 to 40 degrees), which then produces wedging, inclined transverse cracks, and longitudinal cracks.

If inadequate confinement is provided, bond failure would occur as soon as the cracks spread through the concrete cover of the bar. With proper confinement the bond stress reaches a maximum (around $f_c'/3$ according to Reference 6) before decreasing as the concrete between ribs fails and a frictional type of behavior ensues (Figure 2).

## ANALYTICAL REPRESENTATION OF BOND

In finite element analysis of reinforced concrete, bond-slip between reinforcement and concrete has been modeled using interface elements. Interface elements typically use empirical, nonlinear bond stress-slip relationships.

The simplest interface element is the bond-link element (Ref 9, 10, and 11). This is a dimensionless element that connects two nodes with identical coordinates. It can be viewed as consisting of two orthogonal springs between the two nodes. More complex models combine the reinforcement and adjacent concrete into a finite bond-zone element (Ref 12), or represent the interface with a dimensionless contact element that gives a continuous connection between two adjacent elements (Ref 13 through 18). Bond models of the embedded type also have been considered (Ref 19 and 20).

In all these models, the radial stiffness of the interface is an important variable and was included in their development. However, in practical examples, large, arbitrary values of the radial stiffness have been prescribed in the absence of experimental data (Ref 9 and 16). Alternatively, bond modeling has just been avoided (Ref 15 and 21).

With respect to the sensitivity of the finite element model to the longitudinal bond stress versus slip relationship employed, Reference 15 shows variations in rebar stresses of up to 20 ksi (in a Grade 60 bar) depending on which of four different empirical relationships was prescribed.

## EXPERIMENTAL BACKGROUND

In spite of its importance, only a limited amount of research has included radial stress or deformation as a parameter (Ref 22 through 29). Typically, a specimen configuration is chosen and no attempt is made at evaluating the normal stiffness of the reinforced or unreinforced concrete surrounding the bar. As a result very disparate relationships for bond stress versus slip have been obtained (e.g., see Ref 1 and 15), with variations in bond stress over 100 percent.

The main studies that have addressed transverse confinement provide insight into its effects on bond.

Untrauer and Henry (Ref 22) pulled No. 6 and No. 9 Grade 60 bars from 6-inch cube specimens subjected to lateral pressure on two opposite faces. The normal pressure on the specimens was increased up to 2370 psi. They observed an increase in bond strength approximately proportional to the square root of the normal pressure.

Doerr (Ref 23) subjected 16 mm (0.63 in.) deformed bars embedded in a 3-inch diameter cylindrical concrete specimen to tension. The specimen was subjected to confining pressure of up to 15 N/mm$^2$ (2175 psi). It was found that the bond stresses could be incremented up to 50 percent. Doerr also attributed the large scatter in bond stress results reported in the literature to the various dimensions of test specimens used.

Robbins and Standish (Ref 24) pulled 8 and 12 mm (0.31 and 0.47 in.) bars from 100 mm (4 in.) cubes laterally loaded on two opposite faces. The pull-out load for the deformed bars increased more than 100 percent for lateral pressures of about 10 N/mm$^2$ (1450 psi). Additional application of lateral pressure up to 28 N/mm$^2$ (4060 psi) did not increase the failure loads.

Eligehausen, et al. (Ref 25) tested 125 pull-out specimens consisting of a Grade 60 bar with a short length (5 bar diameters) embedded in a 12-inch by 7 $d_b$ by 15 $d_b$ reinforced concrete specimen ($d_b$ being the bar diameter). A unidirectional confining pressure was applied perpendicular to the longitudinal splitting plane. An increase in the confinement from 0 to 1900 psi yielded a 25 percent increase in maximum bond resistance. However, the confinement provided by the transverse steel across the crack plane was not evaluated.

Navaratnarajah and Speare (Ref 26) report an increase in bond performance with increasing lateral pressure up to a limiting value of the lateral pressure.

Gambarova, et al. (Ref 27) pulled 18 mm (0.70 in.) bars embedded in a cracked concrete specimen. External confinement perpendicular to the longitudinal cracking plane allowed control of the longitudinal crack opening, which was kept constant during each test. It was observed that bond increases with increasing confinement, i.e., with decreasing crack opening, by up to 40 percent.

Giuriani, et al. (Ref 29) consider confinement exerted not only by lateral external loads but also by transverse reinforcement and by residual tensile stresses across the concrete cracks.

## BOND-SLIP VARIABLES

It is hypothesized that together with bond stress and longitudinal slip, radial confinement stress and radial deformation are the main variables defining bond behavior. This is apparent in the following observations from experimental bond tests.

- If confinement is not provided, the bond stress vanishes as soon as the longitudinal crack develops through the cover.
- The concrete cover itself provides confinement through tensile hoop stresses prior to cracking.
- The ultimate resistance at large slips is of the Coulomb friction type (see Figure 2).
- Bond stress is higher when bars are pushed instead of pulled. This is due to Poisson's effect: A bar in compression will expand radially, and increase the normal radial stress, thus increasing the bond stress. Vice versa, a bar in tension will shrink and offer less resistance to pull-out.
- The discrepancy in bond stress-slip relationships appearing in the literature would be explained by the variations in the test specimens which provide varying degrees of confinement, and were not accounted for in deriving the relationships.
- Effects of concrete cover, bar spacing, bar position, end distance, and tie confinement could be predicted via the available confinement.

These observations motivated the design of a new testing device and specimen that allow for the control and measurement of the four variables identified.

## STEEL-CONCRETE INTERFACE

Although most analytical representations of bond tend to model the steel to concrete interface as a two dimensional surface, the bond transfer mechanism actually occurs in a finite zone surrounding the rebar (Ref 8 and 12). From an experimental point of view, this means a process zone surrounding the rebar has to be defined, and the slip measured will actually include the deformation of this zone. If the analytical model of the interface has zero thickness, its characteristics will have to be derived indirectly by reproducing the measured bond-slip at the specified distance from the bar.

## TEST SPECIMEN

The process zone chosen for this investigation is shown in Figure 3. It consists of a 3-inch diameter, 4-inch long concrete cylinder surrounding a steel rebar. The cylinder diameter was the smallest practical size for use with pea gravel (Table 1). In an attempt to obtain local characteristics, only five lugs were in contact with the concrete. Contact was prevented in the rest of the specimen by inserting silicone rubber spacers around the bars. The spacers allowed inclined radial cracks forming at each rib to propagate to the outer concrete surface. The outer concrete surface was surrounded by a threaded steel pipe that carried the shear stresses. Figure 4 shows the steel pipe, the steel bar with the test zone delimited by the spacers, and the wood form that was inserted inside the pipe and held the bar in position during casting. Most of the steel pipe was split longitudinally into eight strips in order to prevent any confinement from the pipe itself. The strips' thicknesses were further reduced to increase their flexibility. Figure 5 shows the assembled arrangement. The wood form was removed before testing.

## TEST SETUP

The specimen was installed in a MTS servo-controlled hydraulic testing machine used in displacement control. The bar end was threaded and held fixed. On the other end, the inside of the pipe was threaded and bolted to the piston. The pipe was cut into eight strips as shown in Figures 4 and 5. These strips were very flexible and do not provide any confinement of their own. This was verified experimentally by pulling laterally on the strip's end and measuring force and displacement. The lateral stiffness was determined to be 9 lb/in. During the tests the maximum radial displacement obtained was in the order of 0.02 inch, resulting in an equivalent confining pressure due to the strips of less than 0.12 psi.

Confining pressure was applied through a thin (0.062 inch) ring surrounding the pipe (Figure 5). A hydraulic jack with an adjustable relief valve closed the ring with a constant force during the test. The general setup is shown in Figure 6.

## INSTRUMENTATION

One Linear Variable Differential Transformer (LVDT) measured the slip between the rebar (1/4 inch away from the concrete face) and the outer concrete surface. Another LVDT measured the opening of the confining ring. This was later translated into a radial deformation. The MTS load cell provided pull-out load measurements from which bond stresses were calculated. A pressure gage was used to set the confining pressure, which remained constant for each test.

## PROCEDURE

### Confining Pressure

For Tests P0, P1, and 1 through 5, once the specimen was installed in the loading frame, a confining pressure was set and maintained throughout the test. After longitudinal cracking, the confining pressure on the outer surface of the split pipe transfers directly to the bar surface. The post-cracking confining pressure at the surface of the bar was set at 500, 1500, 2500, 3500, and 4500 psi. The equivalent confining pressures on the outer surface of the 3-inch diameter concrete cylinder are 125, 375, 625, 875, and 1125 psi over a five-lug length (or 82, 246, 410, 574 and 738 psi over the 4-inch length).

For Tests 6 through 10, cracking was obtained for a 500 psi bar level confining pressure. In the post cracking range the same bar level pressures of 500 to 4500 psi were applied to Specimens 6 through 10 respectively.

### Pull-Out Load

All tests were carried out in displacement control to obtain the unloading branches of the responses. The displacement rate was approximately 0.015 in./mn for the first loading, after which it was increased to about 0.075 in./mn.

For the preliminary tests (P0 and P1), the specimens were loaded monotonically to failure. It was observed that the longitudinal splitting crack formation was accompanied with a temporary steep decrease in bond (Test P1). The cracking loads are also dependent on the amount of concrete surrounding the bar.

In order to obtain data independent from the amount of concrete, it was decided to unload the specimens just after the splitting crack formation, then reload them. Hence, for Tests 1 through 10, each specimen was loaded monotonically until longitudinal cracks formed, then completely unloaded, then reloaded until the slip reached approximately 12 mm (1/2 in.).

## EXTERNALLY APPLIED CONFINEMENT

In the previous section the confining pressures at the bar surface for longitudinally cracked were reported as 500, 1500, 2500, 3500, and 4500 psi. For uncracked concrete these values are actually different. For a thick, uncracked concrete cylinder of unit length with a solid steel core (Figure 7a), the concrete stresses are given by (neglecting tangential bond stresses):

$$\text{hoop stress} \quad \sigma_t = \frac{(r_s^2 p_s - r_c^2 p_c) + (p_s - p_c) r_s^2 r_c^2/r^2}{r_c^2 - r_s^2} \tag{1}$$

$$\text{radial stress} \quad \sigma_r = \frac{(r_s^2 p_s - r_c^2 p_c) - (p_s - p_c) r_s^2 r_c^2/r^2}{r_c^2 - r_s^2} \tag{2}$$

which at $r = r_s$ becomes:

$$\sigma_t = \frac{p_s(r_c^2 + r_s^2) - 2 p_c r_c^2}{r_c^2 - r_s^2} \tag{3}$$

$$\sigma_r = - p_s \tag{4}$$

At $r = r_s$, the internal radius of the concrete cylinder increases by:

$$\Delta r_c = r_s(\sigma_t - \mu_c \sigma_r)/E_c \tag{5}$$

$$= \frac{r_s p_s}{E_c(r_c^2 - r_s^2)}\left[r_c^2(1 - \mu_c) + r_s^2(1 - \mu_c) - 2 r_c^2 p_c/p_s\right] \tag{6}$$

The steel core under pressure reduces its radius by:

$$\Delta r_s = r_s p_s(1 - \mu_s)/E_s \tag{7}$$

From Equations 6 and 7:

$$\Delta r_c = - \Delta r_s$$

which yields:

$$p_c/p_s = \frac{1}{2}\left[(1 + \mu_c) + \frac{r_s^2}{r_c^2}(1 - \mu_c) + \frac{E_c}{E_s}(1 - \mu_s)\left(1 - \frac{r_s^2}{r_c^2}\right)\right] \tag{8}$$

This equation holds only for the linear range of the concrete in compression and in the absence of splitting cracks.

For the special case when both materials are the same, Equation 8 reduces to:

$$p_c/p_s = 1 \tag{9}$$

independently of $r_s/r_c$. This is a case of isotropic compression on a homogeneous cylinder.

For the case where $E_c = 4{,}000$ ksi, $E_s = 29{,}000$ ksi, $\mu_c = 0.2$, $\mu_s = 0.3$, $r_c = 1.5$ inch, and $r_s = 0.375$, Equation 8 yields:

$$p_s = 1.49\, p_c \tag{10}$$

These equations were derived for a specimen of unit thickness. For the actual tests, the embedded bar length was five-lug spacings (2.625 inches if a maximum spacing of 0.525 inch is assumed) whereas the concrete cylinder length was 4 inches yielding:

$$p_{st} = 1.49\,(4/2.625)\,p_{ct} = 2.27\,p_{ct} \tag{11}$$

where the subscript t refers to test values.

However, if the concrete is longitudinally cracked and no stresses are transferred across the cracks (Figure 7b), then for a unit thickness specimen:

$$\begin{aligned} p_s &= p_c\, r_c / r_s \\ &= 4\,p_c \end{aligned} \tag{12}$$

and for the present tests

$$p_{st} = 6.1\,p_c \tag{13}$$

During tests where longitudinal splitting has not occurred, Equation 11 indicates the confining pressure at the bar level $p_{st}$ due to the externally applied pressure. During the reloading cycle, after cracking has occurred, Equation 13 holds. In all figures it was decided to show the "nominal" values of $p_{st}$ for cracked state (500, 1500, 2500, 3500, and 4500 psi) from Equation 13.

## PRECRACKING CONCRETE CONFINEMENT

Prior to cracking, the concrete specimen itself provides some confinement via tensile hoop stresses. The confining stress due to the concrete cylinder just before cracking (in the absence of external forces and for unit thickness) can be evaluated from Equation 3 by setting $\sigma_t = f_t$ and $p_c = 0$, yielding:

$$p_s = \left( \frac{r_c^2 - r_s^2}{r_c^2 + r_s^2} \right) f_t \tag{14}$$

For Test P0 (no external confinement) and a five-lug embedded length

$$p_s = 1061 \text{ psi} \tag{15}$$

The magnitude of the confining stress due to the concrete cylinder is within the range of the externally applied confining stresses.

Total confinement prior to cracking is therefore variable, and is a combination of the concrete cylinder confinement and the externally applied one. After cracking, the total confining stress is constant and only Equation 13 is needed to obtain it. This explains the emphasis of the present study on the post-cracking behavior.

## TEST SERIES

Three test series were carried out. The first series (preliminary Tests P0 and P1) were carried out to verify the setup. No confining pressure was applied for Test P0.

For the first and second test series (Tests P0, P1 and 1 through 5), bars with inclined ribs that formed a 68 degree angle with the longitudinal axis were used. For a No. 6 bar, the maximum rib spacing was 13.3 mm (0.525 inch). The measured rib spacing was 12.2 mm (0.481 inch), and the clear distance between ribs was 9.2 mm (0.36 inch).

For the third test series (Tests 6 through 10), bars with normal ribs at an angle of 90 degrees with the bar axis were used. The measured rib spacing was 12.8 mm (0.504 inch), and the clear distance between them was 10.2 mm (0.40 inch).

In all cases, Grade 60, No. 6 bars satisfying ASTM A615-89 were used. The same concrete mix was used in all cases (Table 1). Concrete properties for each series of tests are indicated in Table 2. Compressive strength and tensile splitting strength at 28 days were obtained from three cylinders each. The concrete cylinders were 3 inches in diameter and 6 inches tall.

## RESULTS

### Tests P0 and P1

The first preliminary test, P0, was carried out with no confinement to provide a baseline bond-slip relation for the effect of confinement. Test P1 was run with 1000 psi confinement stress at the bar surface level to show the effect of confinement. Both tests are detailed in Figure 8 (expanded ascending branch) and Figure 9 (complete test results).

For Test P0, Figure 9 shows a dashed segment that is only meant to indicate the beginning and end of the sudden splitting crack propagation. For Test P1, Figure 9 shows the sudden decrease in bond stress at the formation of the longitudinal splitting crack.

### Tests 1 Through 5

Figure 10 shows bond-slip prior to and up to longitudinal cracking. When cracking occurred, 0.1 to 0.2 mm slips took place at almost constant load. The specimens were then unloaded and reloaded. Upon unloading, residual slips of 0.18, 0.10, 0.20, 0.26, and 0.17 mm were measured, for Tests 1 through 5 respectively. Figure 11 shows the post-cracking reloading bond-slip behavior.

Figures 12 and 13 show the bond stress versus slip reloading relationship after longitudinal cracking had taken place on two different scales. Figure 14 indicates the radial displacement at the outer surface of the 3-inch concrete cylinder.

Figure 15 shows a typical specimen failure (Test 4). Both longitudinal and inclined transverse (radial) cracks can be seen. Crushed concrete is present in between the ribs. As the confining pressure was increased, the radial cracks became more prominent as shown by Specimen 5 on Figure 16.

### Tests 6 Through 10

Test 6 was successfully completed at a constant confining load during pre- and post-cracking. For Test 7 (confining pressure 1000 psi) the radial cracking became so severe that slippage began to take place between the concrete specimen and the outer split pipe. The failed specimen is shown in Figure 17. Results from this specimen were discarded and it was decided to pre-crack the remaining specimens at the lowest confining pressure (500 psi). As a consequence no results were obtained for the pre-cracking bond-slip relationships as a function of confining stress. When the pre-cracking cycle was completed, residual slips of 0.054, 0.057, 0.064, and 0.100 mm were observed for Tests 6, 8, 9, and 10 respectively.

The initial post-cracking relationships for various confinement pressures are detailed in Figure 18. Figure 19 shows the complete post-cracking bond stress versus slip relationship.

Figure 20 indicates the radial displacement at the outer surface of the 3-inch concrete cylinder. Figure 21 shows the crack patterns for this series and Figure 22 shows a typical specimen in this series (Test 9).

## DISCUSSION

### Preliminary Tests

Test P0 verifies that (1) without confinement, bond is totally lost very early on, and (2) the eight strips in which the pipe is split provide almost negligible confinement, as indicated in Figure 9.

### Pre-cracking Loading

For Tests 3, 4, and 5 (Figure 10) the curves are very similar. Tests 1 and 2 are close to each other but differ from the others in their initial stiffness. For Tests P0 and P1 (Figure 8) the two curves fall within the scatter of Tests 3, 4, and 5.

With respect to the cracking load, there appears to be a trend of higher cracking loads for higher confinement, although there is also considerable scatter.

The scatter in the loading curves and their little initial differentiation for various confining pressures may be attributed to the following.

- At the beginning of the pull-out tests a major contribution to the behavior is due to adhesion which is independent of confining pressure.

- At the beginning of the pull-out tests the confining pressures on the bars' surfaces are actually smaller than the "nominal" values since they follow Equation 10 rather than Equation 11.

- Eccentricity or misalignment of the rebar could affect the slip readings by the bar bending close to the concrete face.

- Specimens for Tests 1 and 2 were slightly oversized (3.15- and 3.1-inch diameter instead of 3-inch diameter) and did not fit perfectly in the confining ring.

For Tests 6 through 10 pre-cracking curves were obtained for a single confining pressure and are not reported.

**Post-cracking Initial Loading**

For Specimens 1 through 5 the post-cracking reloading curves (Figures 10 and 11) are very similar to the pre-cracking loading ones. Similar observations are appropriate, except that in the present stage adhesion has been overcome.

**Complete Post-cracking Relationships**

Figures 12, 13, and 19 clearly indicate the effect of confinement on bond stress versus slip. The maximum bond stress attained increases almost linearly with confining pressure. For Test 10, the maximum bond stress is almost three times that for Test 6. The bond stress then decreases until the slip is approximately equal to the clear rib spacing (9.2 mm or 0.36 inch for this rebar). At this point the concrete between ribs was crushed and a Coulomb type friction ensued, with a bond stress proportional to normal stress and independent of slip.

At high confinement (Test 5) the post-peak decay was faster than expected. This is attributed to the faster degradation produced by high confinement and high strain energy density. This seems to indicate the existence of a limiting value of the confining stress beyond which bond behavior is not improved. This is consistent with previous observations (Ref 24 and 26).

For Tests 6 through 10, Figure 19 shows a very similar behavior, including a faster decay at high confinement. For these bars, the clear rib spacing was 10.2 mm (0.40 inch). It should be noticed that although the concrete strength is lower (5570 instead of 5830 psi for Tests 1 through 5), the bond stress is higher, indicating better bond characteristics for normal ribs (at 90 degrees with the bar axis).

**Radial Deformation**

Figures 14 and 20 show the radial displacement of the outer concrete specimen fiber for Tests 1 through 5 and 6 through 10, respectively. It is observed that the radial deformation decreases as confinement stress increases. For Test 1 it is suspected that radial displacement was slightly inhibited by the specimens' oversize. The specimens expand laterally after cracking, reach a fairly constant maximum expansion, then start contracting as the interface between rebar and concrete deteriorates.

**Transverse (Radial) Versus Longitudinal Cracks**

Both types of cracking are always present, as seen in Figures 15, 16, 17, 21, and 22. For Tests 1 through 5, the longitudinal crack rapidly became the most important yielding to the bond failure. At higher loads, however, the radial cracks were getting more and more pronounced. For Test 7, radial cracks overcame the longitudinal ones and started bond failure.

For this type of rebar with normal ribs (at 90 degrees with the rebar axis) the process zone appears to be in excess of the specimens' size. The cracking bond stress appears to be higher and better bond characteristics are apparent. These bars also showed more crushed concrete gathering at the front of the ribs.

## CONCLUSIONS

Twelve specimens consisting of a No. 6 rebar embedded in a 3-inch diameter concrete cylinder were tested under controlled confinement. From the experimental observations on bond-slip behavior, it was concluded that:

1. Consistent bond stress versus slip relationships for a short embedded length can be obtained for various degrees of confining pressure.

2. In the precracking range, influence of confinement stress is suspected but could not be properly established with the present tests. The scatter in the results, particularly in the early stages of loading, are attributed to: the important role of adhesion (prior to cracking), reduced radial confining stress on the bar surface, possible eccentricity or misalignment of the bar, and small variation in the specimen size.

3. In the post-cracking range, confinement stress was clearly influential. Bond stress increased proportionally to the applied confining stress, indicating the necessity of considering radial stress on the bar as a modeling parameter. The maximum bond stress could be increased by almost 200 percent by increasing the confinement stress from 500 to 4500 psi at the bar level. The effect of confinement on bond behavior appeared less pronounced for the highest confining stress.

4. In the post-cracking range, radial deformation measured on the outer concrete surface showed an increase up to a limit value dependent on the confinement level.

5. Bars with normal ribs (at 90 degrees with the longitudinal axis) exhibited better bond characteristics than bars with inclined ribs. Bars with normal ribs also produced more severe radial cracking and generated a wider process zone.

6. Increased radial pressure generated more severe radial cracking.

## CURRENT AND FUTURE WORK

Current analytical and numerical modeling work at the University of California, Davis (Ref 30), indicates that the experimental bond stress-slip relationships obtained can be used to accurately model previous tests with very different specimen configurations, such as the ones reported in References 25 and 27.

Additional tests with preformed cracks would avoid the need for the pre-cracking cycle. Further experimental work is also needed to determine strain rate effects and cyclic behavior.

## ACKNOWLEDGMENTS

Funding for the present study was provided by the Office of Naval Research.

Support provided by Dr. T. Shugar and Dr. G. Warren of the Naval Civil Engineering Laboratory, Port Hueneme, and Professor L. Herrmann, U.C. Davis, is gratefully acknowledged.

## REFERENCES

1. American Society of Civil Engineers. State-of-the-art report: Finite element analysis of reinforced concrete, Task Committee on Finite Element Analysis of Reinforced Concrete Structures, 1982.

2. J. G. Rots. "Bond-slip simulations using smeared cracks and/or interface elements," Research Report 85-01, Structural Mechanics Group, Department of Civil Engineering, Delft University of Technology, Delft, The Netherlands, 1985.

3. _____. Computational modeling of concrete fracture, Ph.D. thesis, Department of Civil Engineering, Delft University of Technology, Delft, The Netherlands, Sep 1988.

4. RILEM Technical Committee 90-FMA. "Fracture mechanics of concrete/applications," Second Draft Report over the State of the Art, Division of Structural Engineering, Lulea University of Technology, S-951 87 Lulea, Sweden, May 1987.

5. L. A. Lutz and P. Gergely. "Mechanics of bond and slip of deformed bars in concrete," Journal of the American Concrete Institute Proceedings, vol 64, no. 11, Nov 1967, pp 711-721.

6. P. Gambarova and C. Karakoc. "Shear confinement interaction at the bar to concrete interface," Proceedings of the Bond in Concrete International Conference, Peisley College of Technology, Scotland, pp 82-96. Applied Science Publishers (P. Bartos, editor), 1982.

7. Y. Goto. "Cracks formed in concrete around deformed tension bars," American Concrete Institute Journal, no. 4, 1971.

8. W. H. Gerstle and A. R. Ingraffea. "Does bond-slip exist?" Micromechanics of Failure of Quasi-Brittle Materials, in Proceedings of the International Conference, Albuquerque, New Mexico, Jun 1990 (S.P. Shah, S.E. Swartz, and M.L. Wang, ed., 1990).

9. D. Ngo and A. C. Scordelis. "Finite element analysis of reinforced concrete beams," American Concrete Institute Journal, pp 152-163, 1967.

10. R. N. Murtha and T. J. Holland. Memorandum to files on the analyses of WES FY82 dynamic shear test structures, Naval Civil Engineering Laboratory, Port Hueneme, Dec 1982.

11. L. R. Herrmann. "Finite element analysis of contact problems," Journal of the Engineering Mechanics Division, American Society of Civil Engineers, vol 104, no. EM5, Oct 1978, pp 1043-1057.

12. A. K. DeGroot, G. M. A. Kusters, and Th. Monnier. "Numerical modelling of bond-slip behavior," HERON, vol 26, no. 1B, 1981, 90 pp.

13. M. Hoshino. Ein beitrag zur untersuchung des spannungszustandes an arbeitsfugen mit spannglied-kopplungen von abschnittweise in ortbeton hergestellten spannbetonbrucken, Dissertation, Technische Hochschule, Darmstadt, Germany, 1974.

14. H. Schafer. "A contribution to the solution of contact problems with the aid of bond elements," Computer Methods in Applied Mechanics and Engineering, vol 6, 1975, pp 335-354.

15. M. Keuser, and G. Mehlhorn. "Finite element models for bond problems," Journal of Structural Engineering, American Society of Civil Engineers, vol 113, no. 10, Oct 1987, pp 2160-2173.

16. M. Keuser, G. Mehlhorn, and V. Cornelius. "Bond between prestressed steel and concrete - Computer analysis using ADINA," Computers and Structures, vol 17, no. 5/6, pp 669-676, 1983.

17. G. Mehlhorn, J. Kollegger, M. Keuser, and W. Kolmar. "Nonlinear contact problems - A finite element approach implemented in ADINA," Computers and Structures, vol 21, no. 1/2, pp 69-80, 1985.

18. G. Mehlhorn and M. Keuser. "Isoparametric contact elements for analysis of reinforced concrete," Finite Element Analysis of Reinforced Concrete Structures, American Society of Civil Engineers. Proceedings of a seminar sponsored by the Japan Society for the Promotion of Science and the U.S. National Science Foundation, Tokyo, Japan, 1985, pp 329-347.

19. R. J. Allwood and A. A. Bajarwan. "A new method for modelling reinforcement and bond in finite element analyses of reinforced concrete," International Journal for Numerical Methods in Engineering, vol 28, 1989, pp 833-844.

20. M. Cervera, E. Hinton, and O. Hassan. "Nonlinear analysis of reinforced concrete plate and shell structures using 20-noded isoparametric brick elements," Computers and Structures, vol 25, no. 6, pp 845-869, 1987.

21. A. H. Nilson. "Nonlinear analysis of reinforced concrete by the finite element method," American Concrete Institute Journal, vol 65, no. 9, Sep 1968, pp 757-767.

22. R. E. Untrauer and R. L. Henry. "Influence of normal pressure on bond strength," American Concrete Institute Proceedings, vol 62, no. 5, May 1965, pp 577-586.

23. K. Doerr. "Bond behavior of ribbed reinforcement under transversal pressure," Nonlinear Behavior of Reinforced Concrete Spatial Structures, IASS Symposium, vol 1, p 13, Werner-Verlag, Dusseldorf, 1978. (G. Melhorn, H. Ruhle, and W. Zerna, ed.)

24. P. J. Robins and I. G. Standish. "Effect of lateral pressure on bond of reinforcing bars in concrete," Bond in Concrete, Proceedings of the International Conference, Peisley College of Technology, Scotland, Applied Science Publishers (P. Bartos, editor), 1982, pp 262-272.

25. R. Eligehausen, E. P. Popov, and V. V. Bertero. "Local bond stress-slip relationships of deformed bars under generalized excitations," Report No. UCB/EERC-83/23, Earthquake Engineering Research Center, University of California, Berkeley, Oct 1983.

26. V. Navaratnarajah and P. R. Speare. "A theory of transfer bond resistance of deformed reinforcing bars in concrete under lateral pressure," Magazine of Concrete Research, vol 39, no. 140, Sep 1987, pp 161-168.

27. P. G. Gambarova, G. P. Rosati, and B. Zasso. "Steel-to-concrete bond after concrete splitting: Test results," Materials and Structures, vol 22, no. 127, Jan 1989, pp 35-47.

28. _____. "Steel-to-concrete bond after concrete splitting: Constitutive laws and interface deterioration," Materials and Structures, vol 22, no. 127, Jan 1989, pp 347-356.

29. E. Giuriani, G. Plizzari, and C. Schumm. "Role of stirrups and residual tensile strength of cracked concrete on bond," Journal of Structural Engineering, American Society of Civil Engineers, vol 117, no. 1, Jan 1991.

30. L. R. Herrmann. Private Communication, Feb 1991.

**Table 1. Concrete Mix**

| Ingredient | Amounts (lb/yd3) |
|---|---|
| Cement | 658 |
| Water | 367 |
| Sand | 1760 |
| Gravel, 3/8-inch | 910 |

**Table 2. Concrete Properties**

| Test | Compressive Strength (psi) | Tensile Strength (psi) |
|---|---|---|
| 0 | 6410 | 723 |
| 1-5 | 5830 | 715 |
| 6-10 | 5570 | 680 |

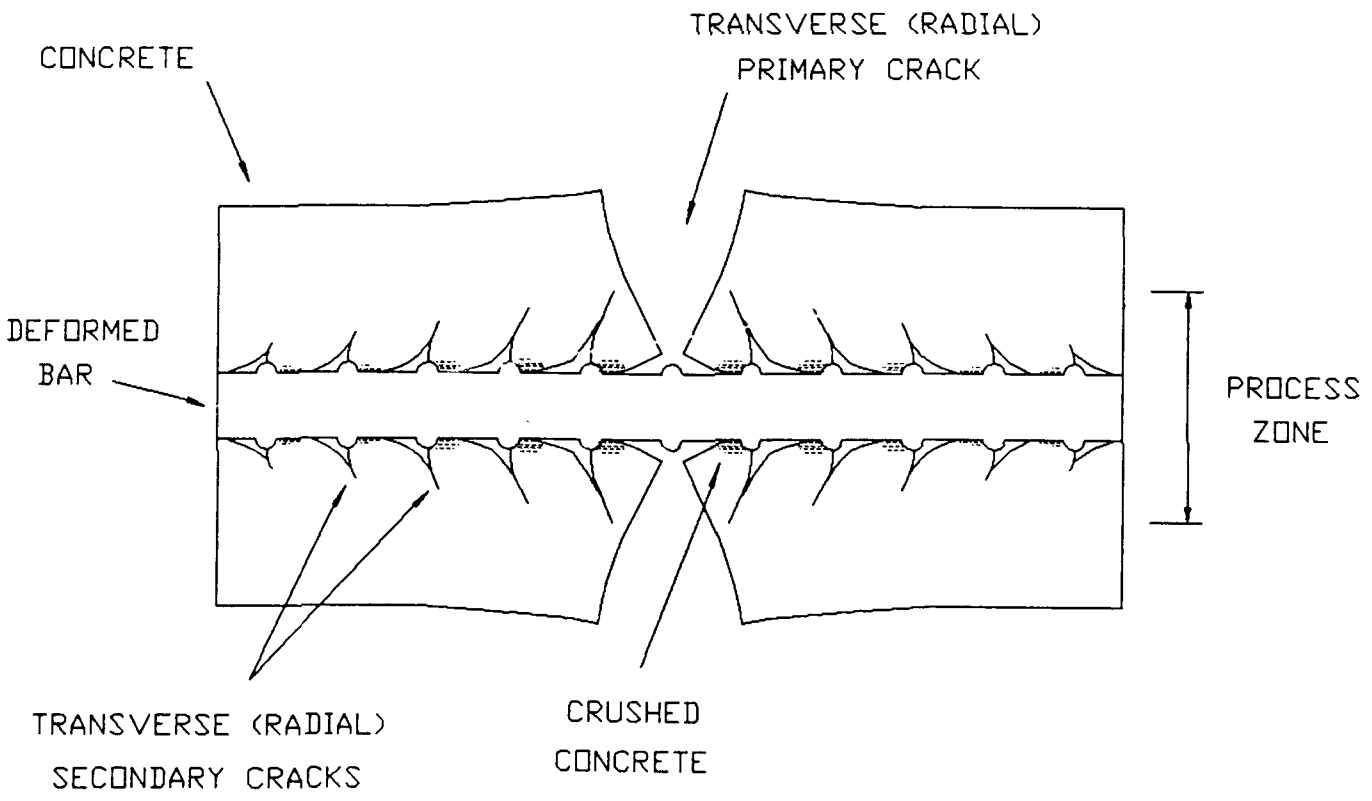


Figure 1.
Bond stress transfer by wedging action.

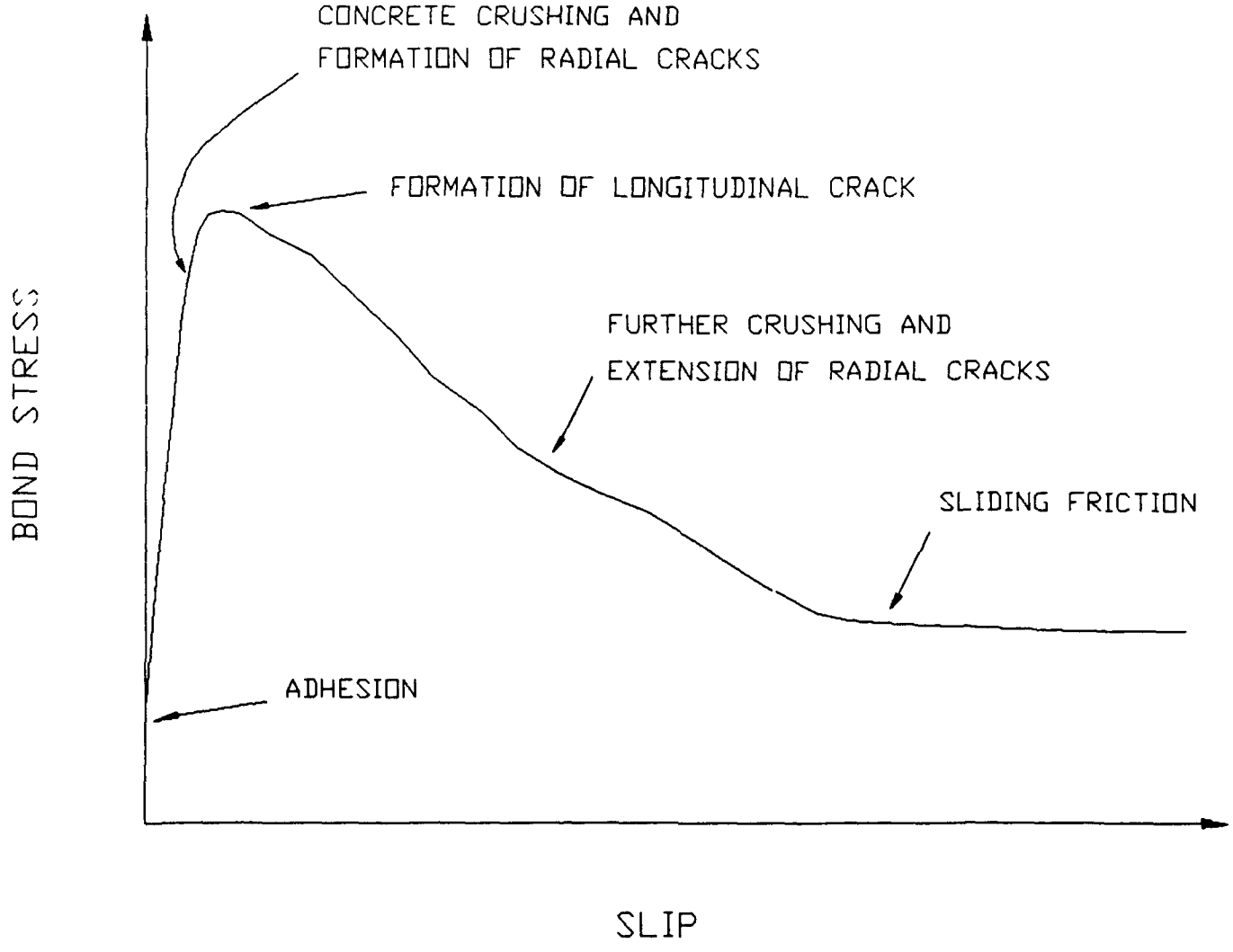


Figure 2.
Typical bond stress-slip relationship.

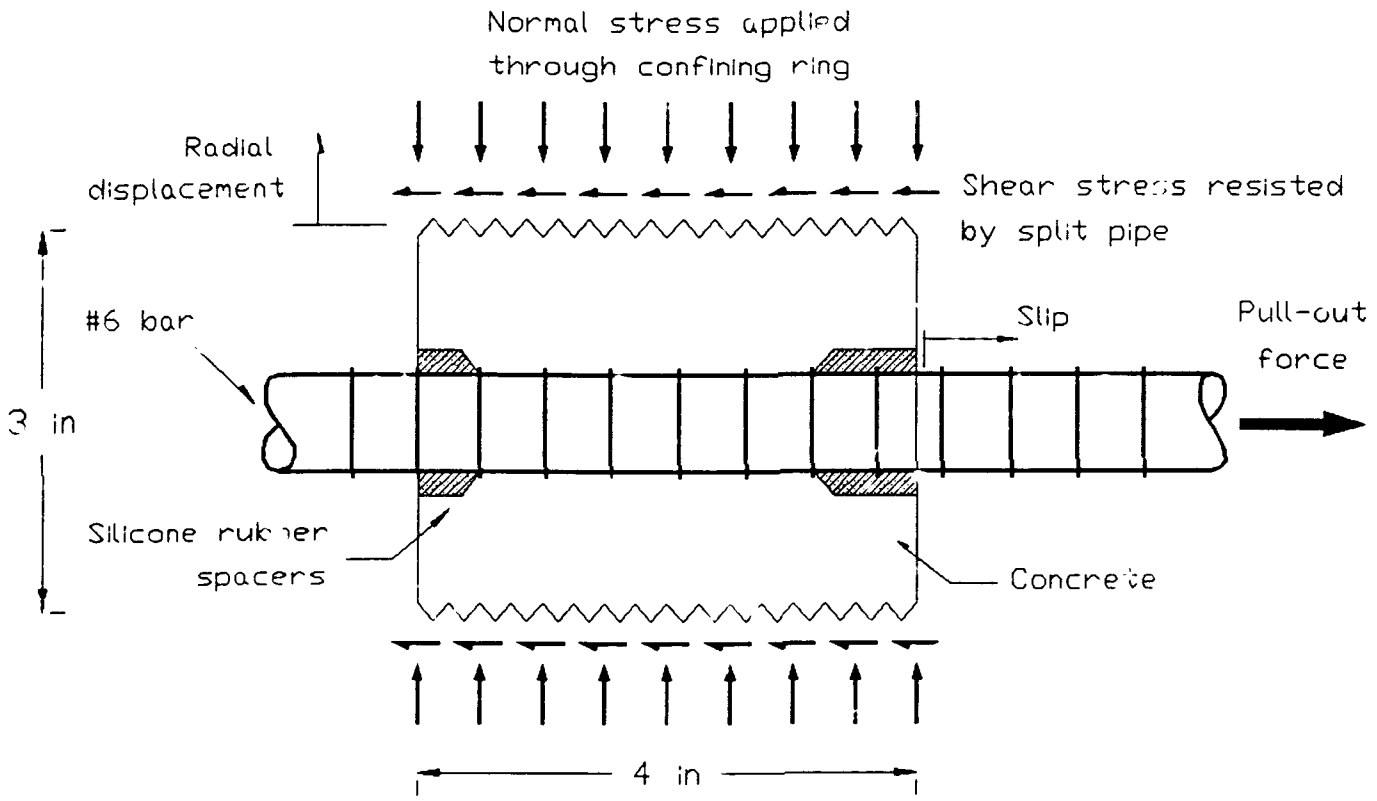


Figure 3.
Test specimen.

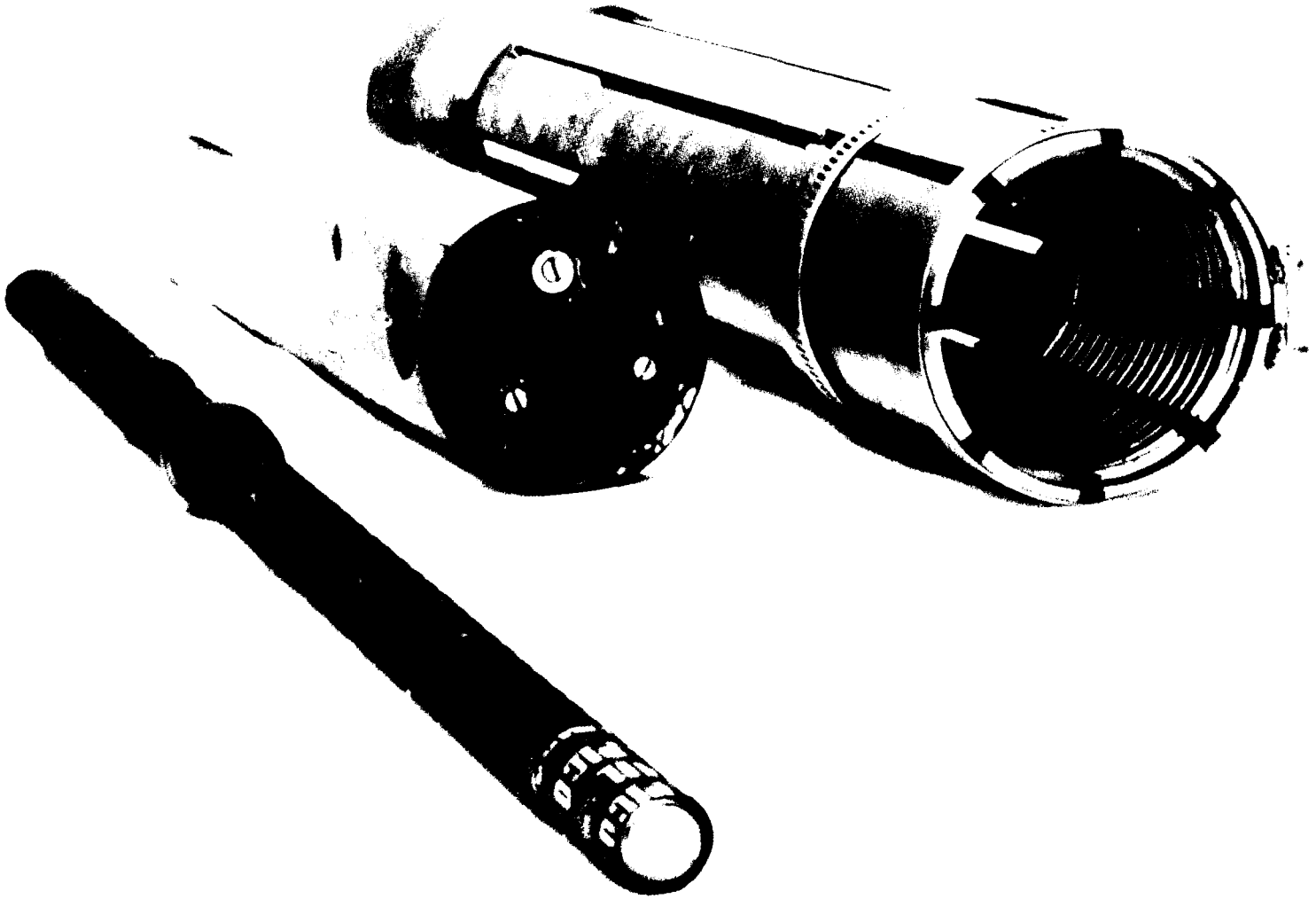

Figure 4.
Test specimen mold.

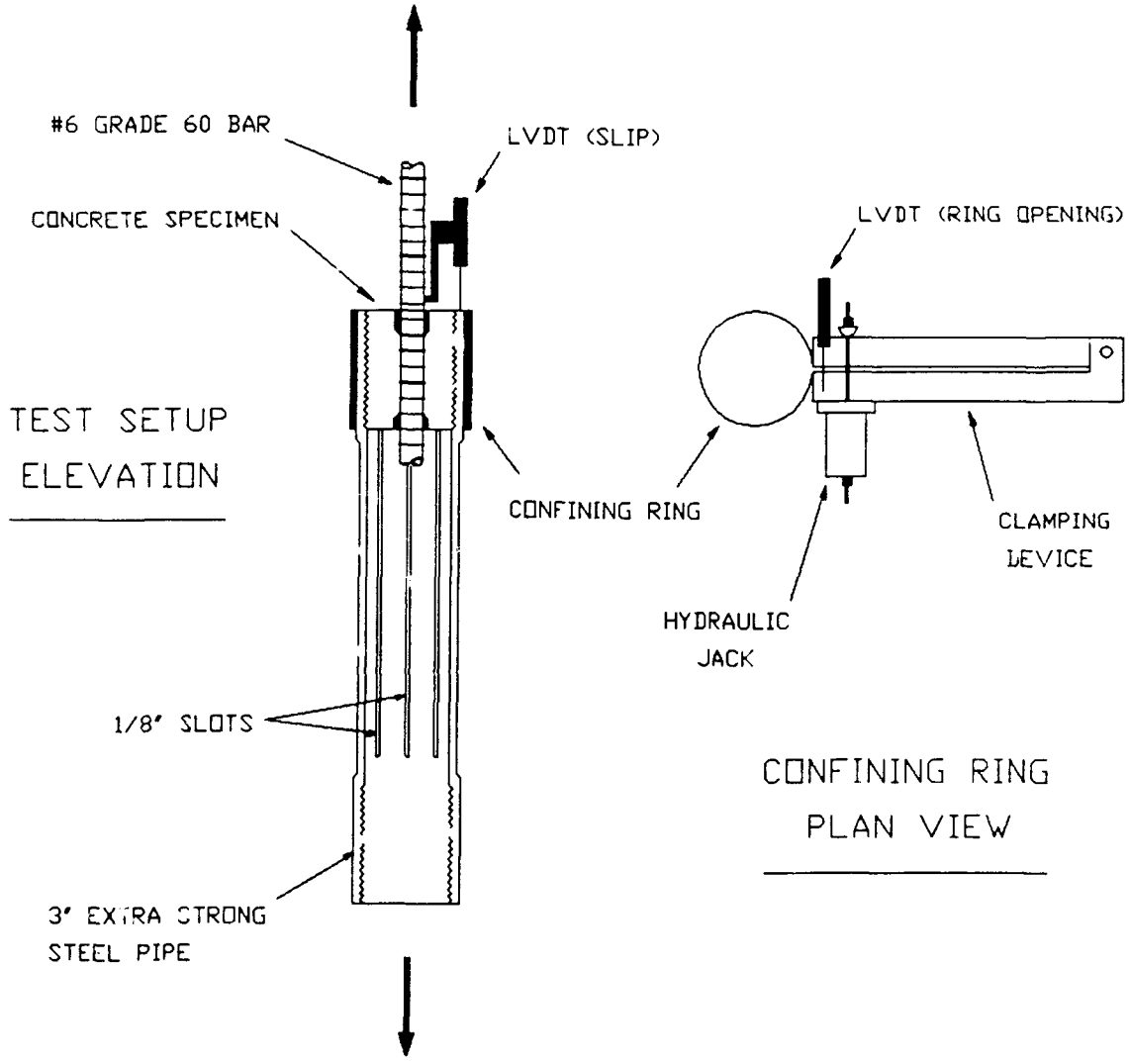


Figure 5.
Testing apparatus and confining ring.

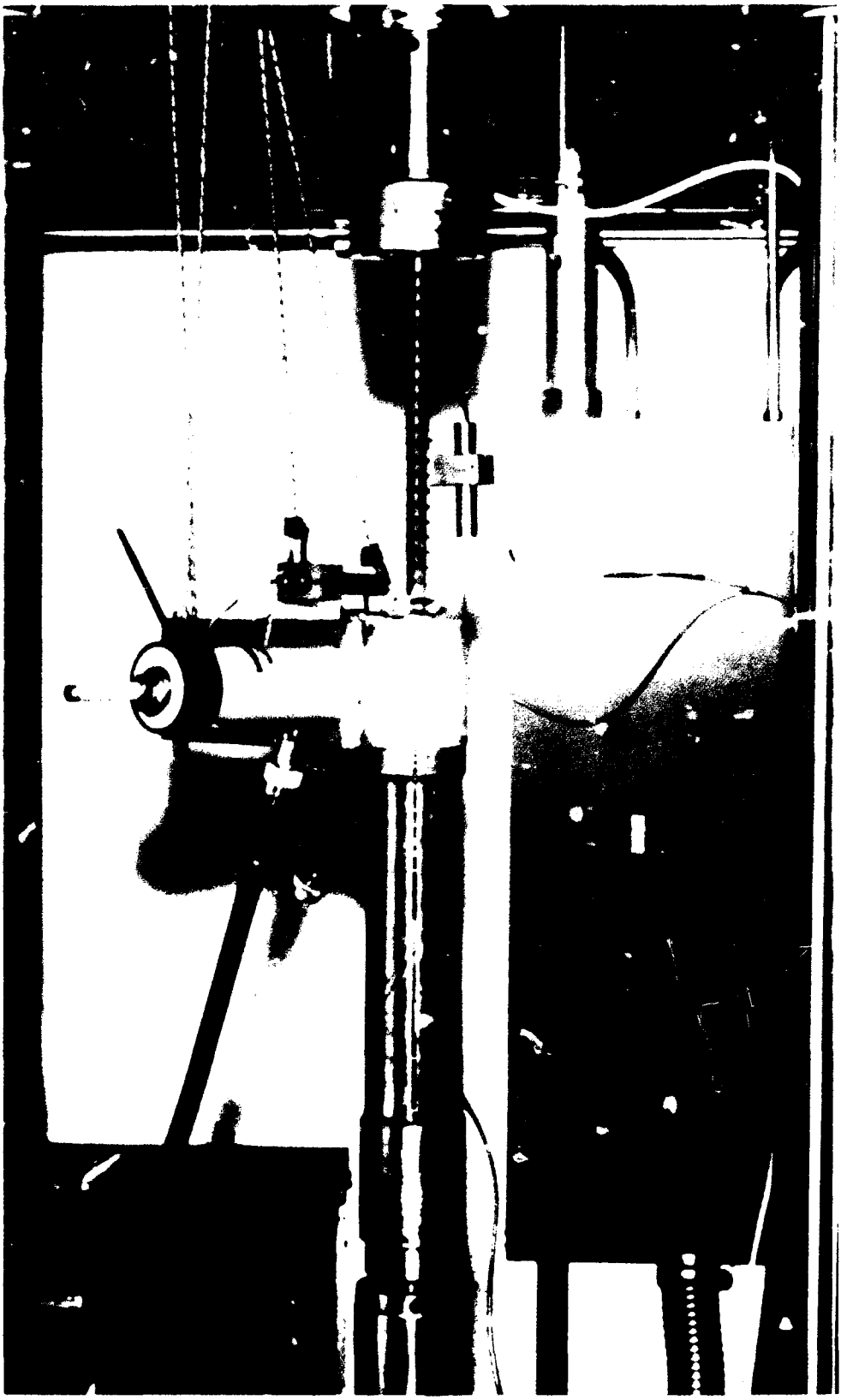

Figure 6.
Test setup and testing machine.

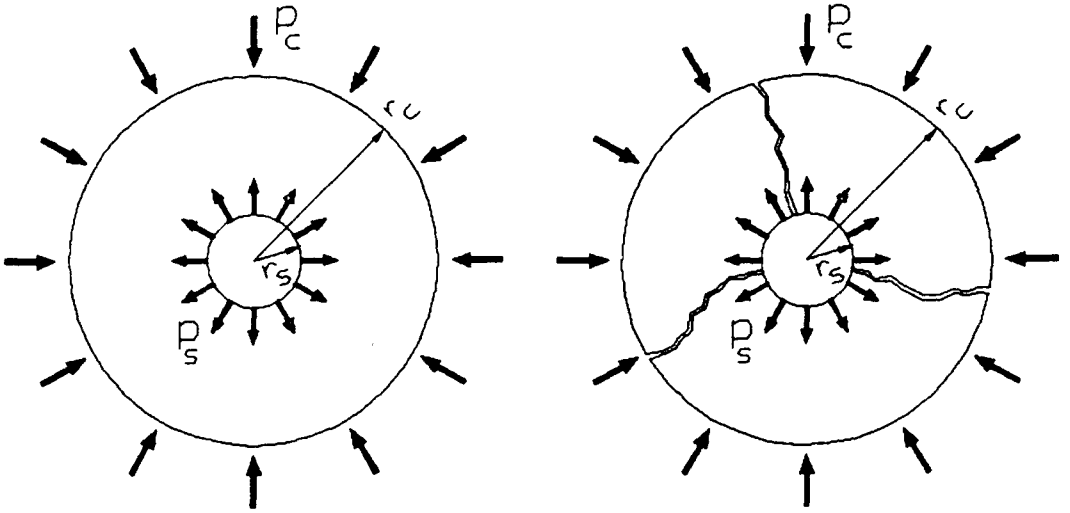


(a) Prior to cracking (b) After longitudinal splitting

Figure 7.
Externally applied confinement.

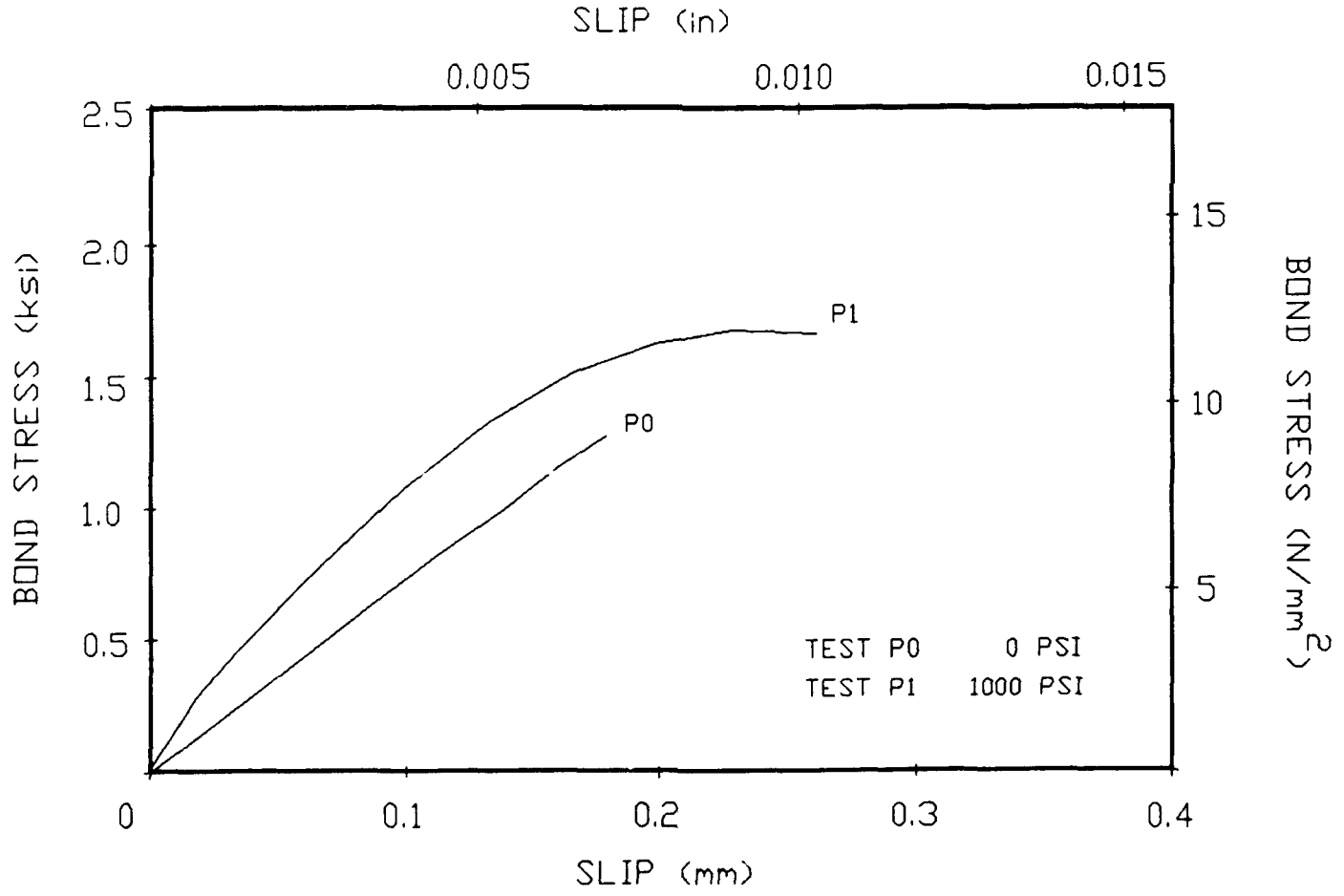


Figure 8.
Preliminary tests: Bond-slip prior to cracking.

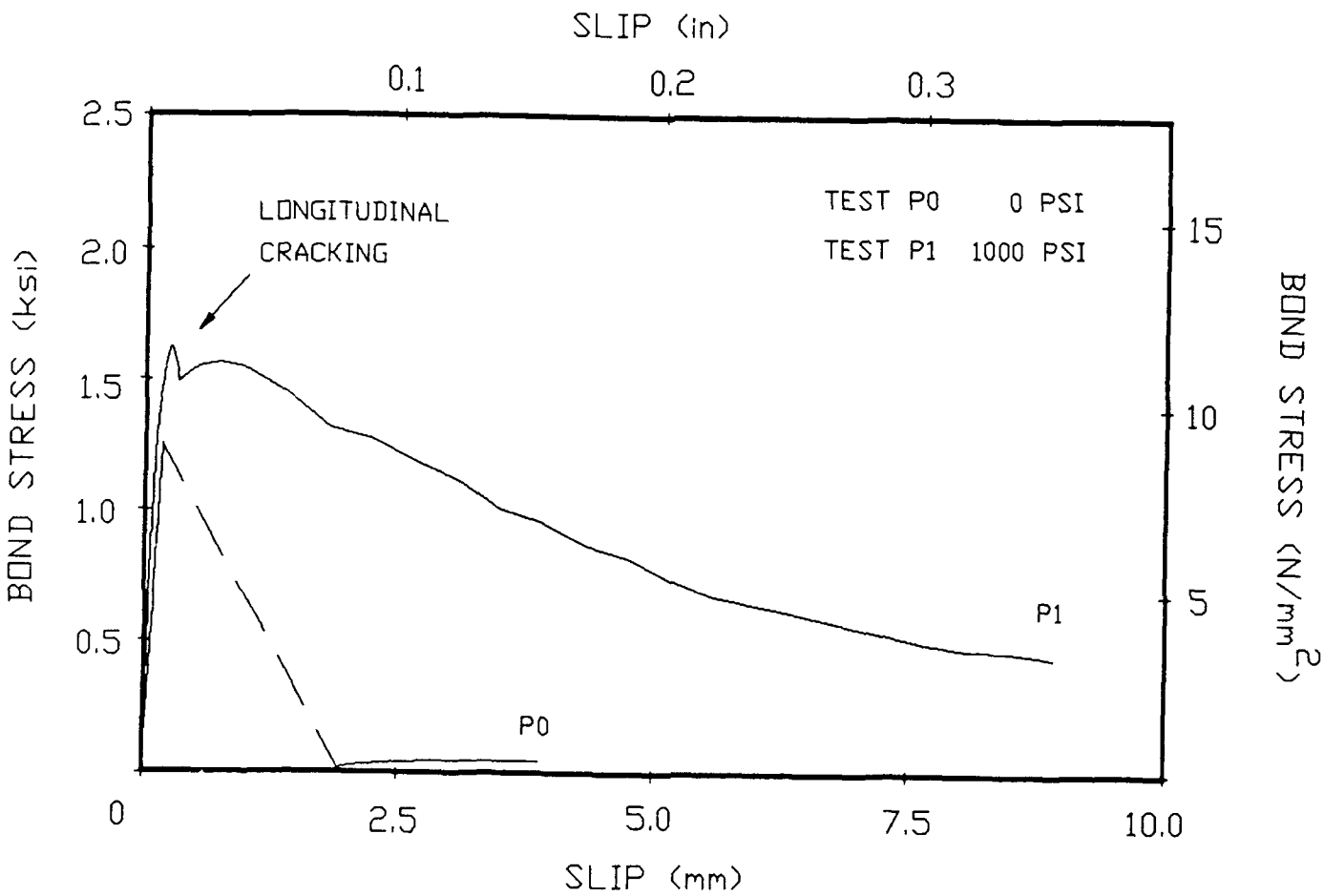


Figure 9.
Preliminary tests: Complete tests.

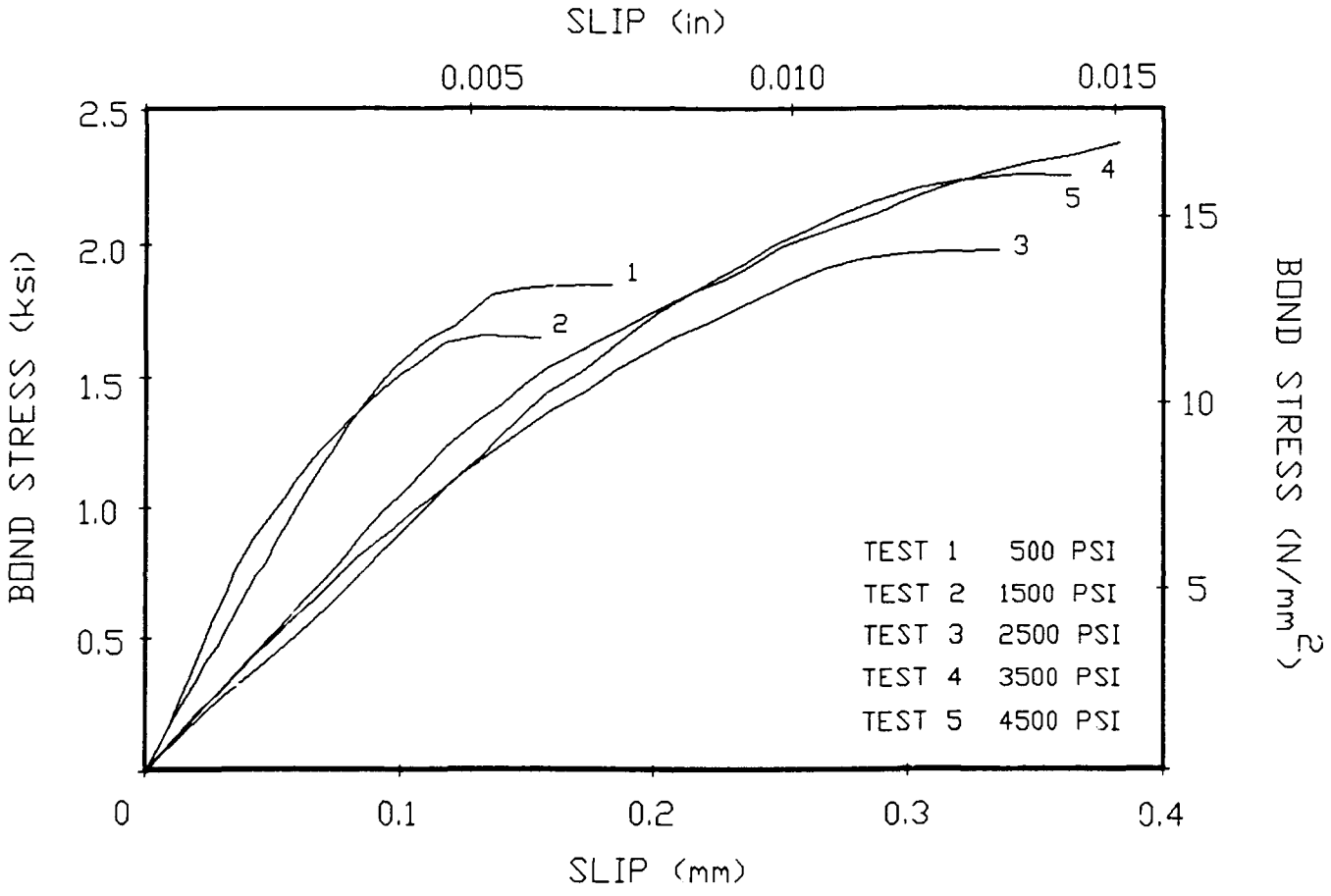


Figure 10.
Tests 1 through 5: Bond-slip prior to cracking.

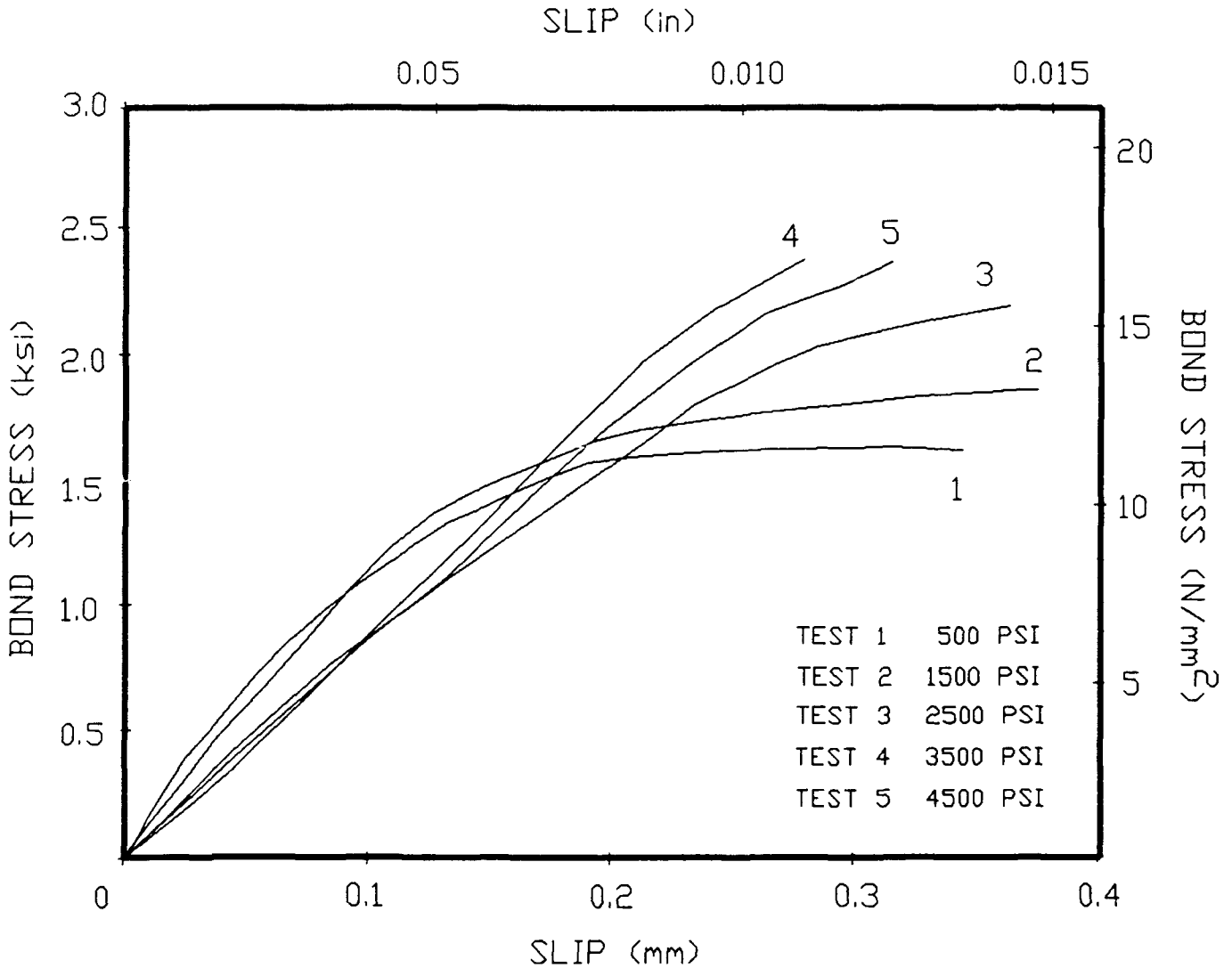


Figure 11.
Tests 1 through 5: Initial post-cracking bond-slip.

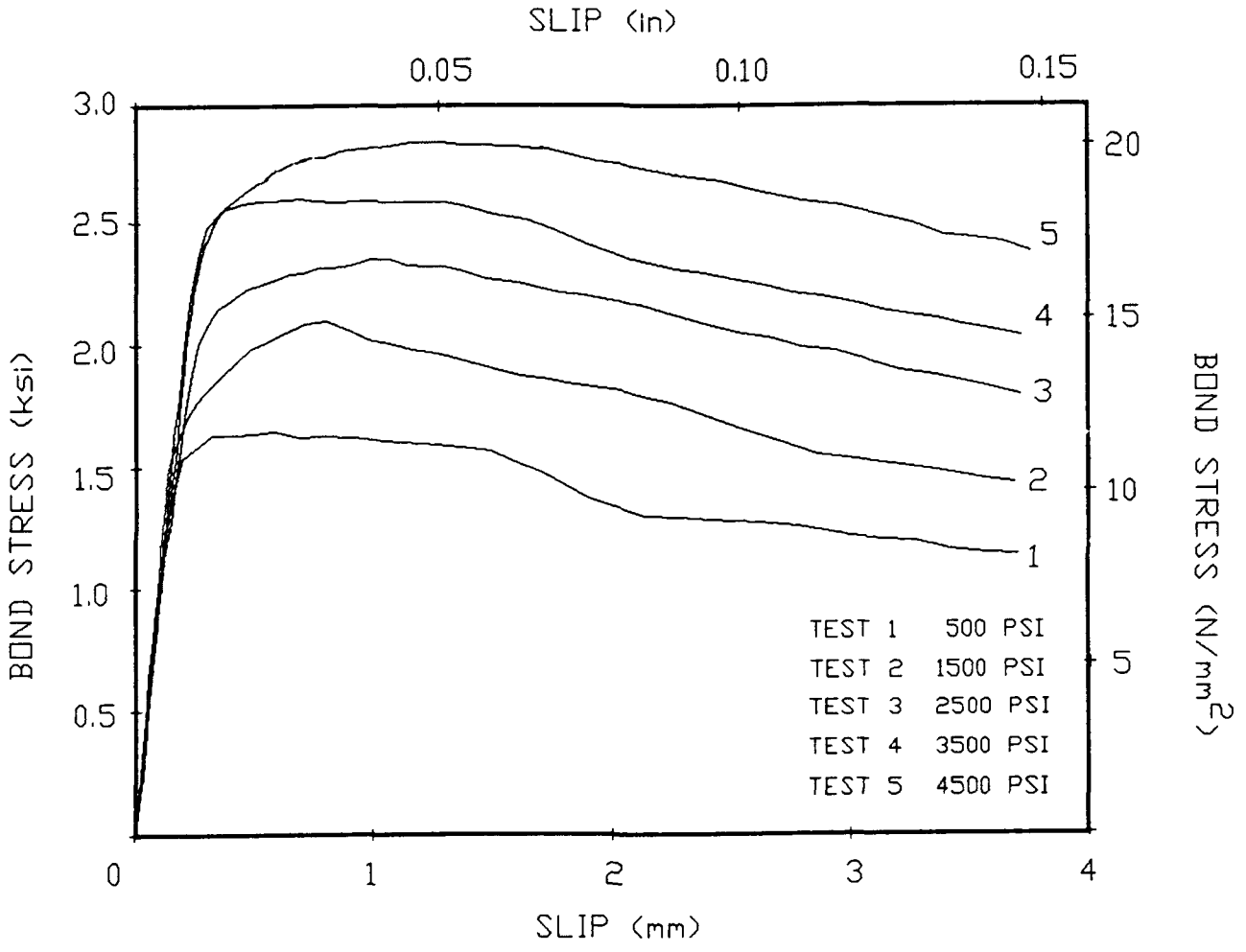


Figure 12.
Tests 1 through 5: Post-cracking bond-slip relationships.

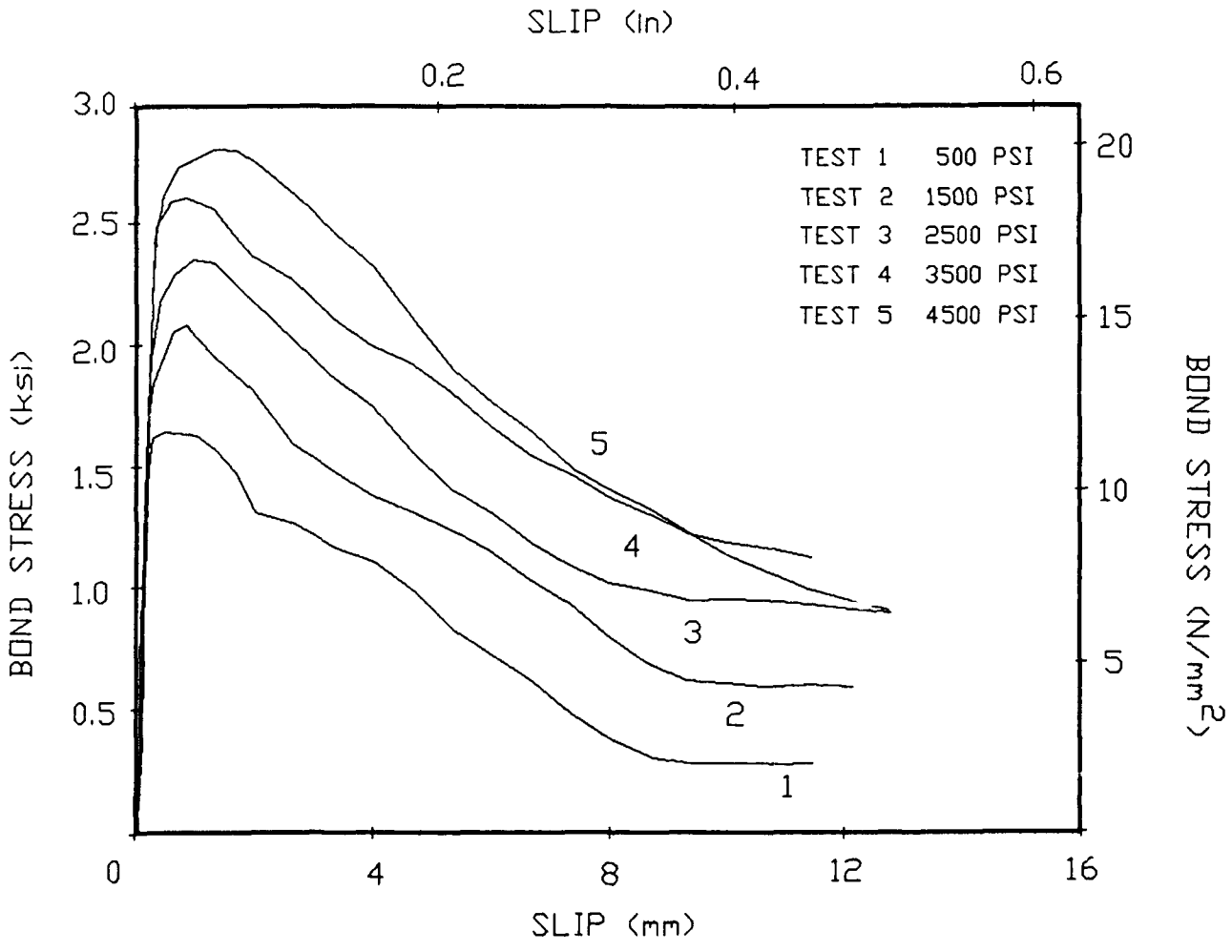


Figure 13.
Tests 1 through 5: Complete bond-slip relationships.

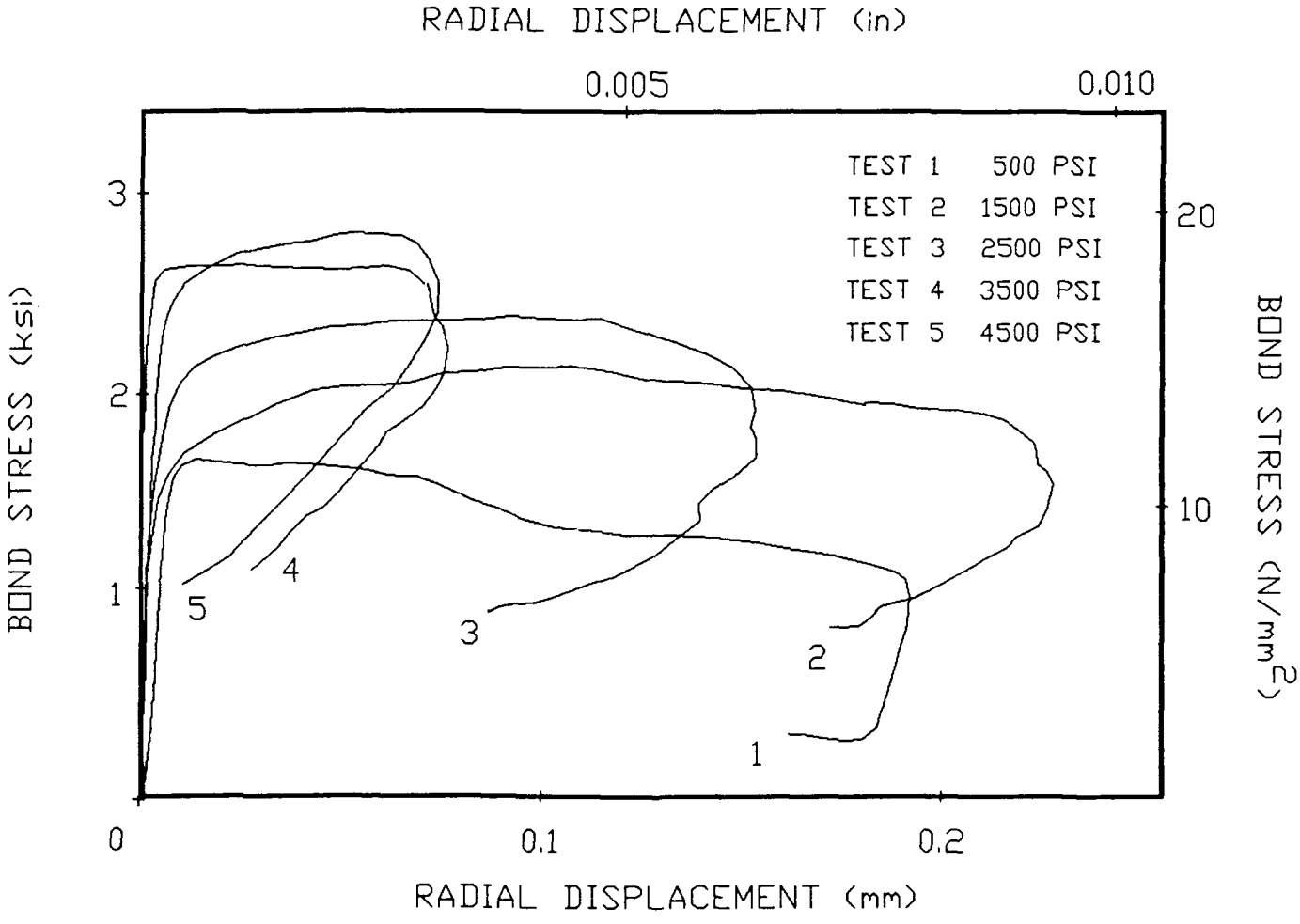


Figure 14.
Tests 1 through 5: Radial displacement histories.

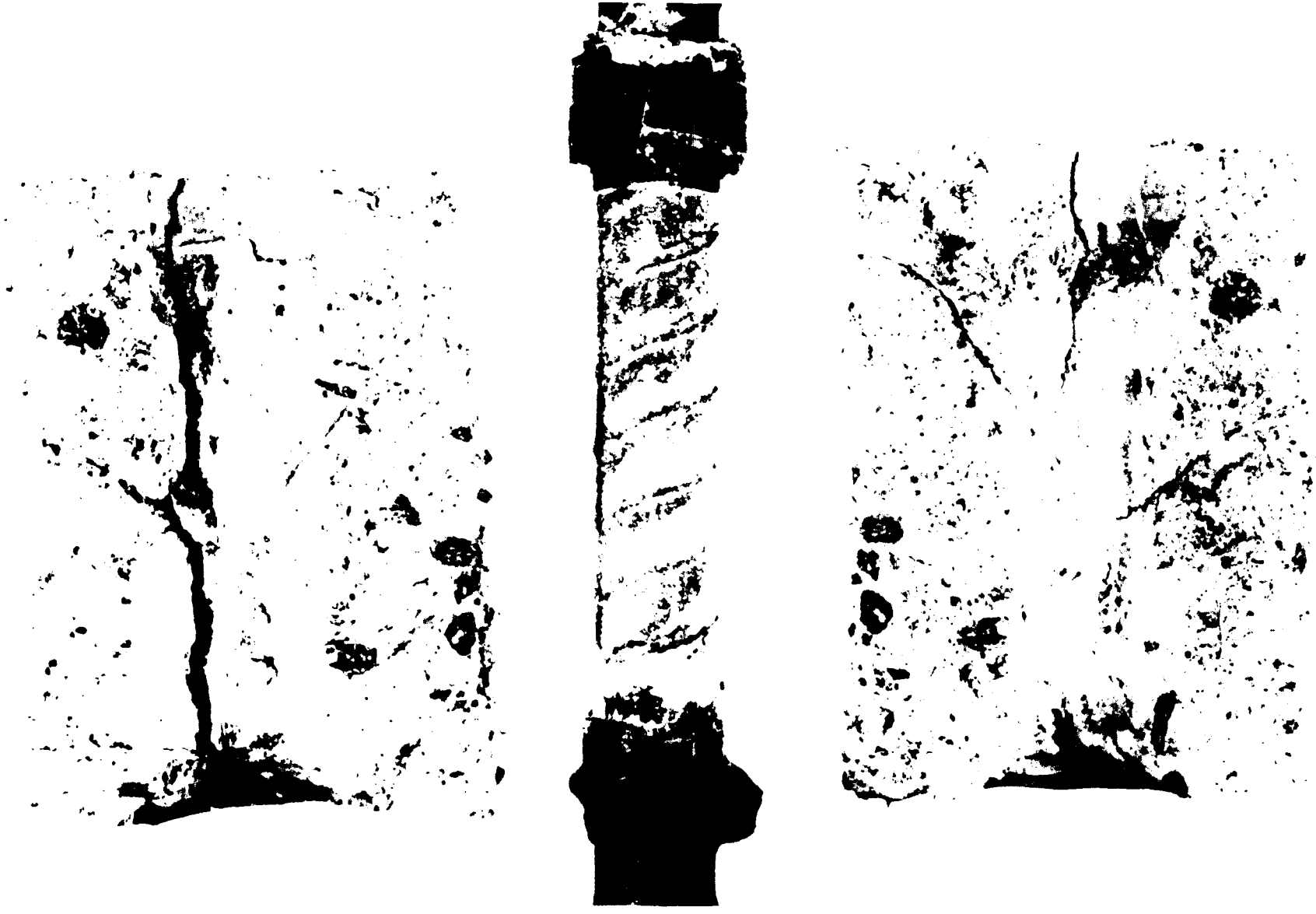

Figure 15.
View of Specimen 4 after failure.

Figure 16.
View of Specimen 5 after failure.

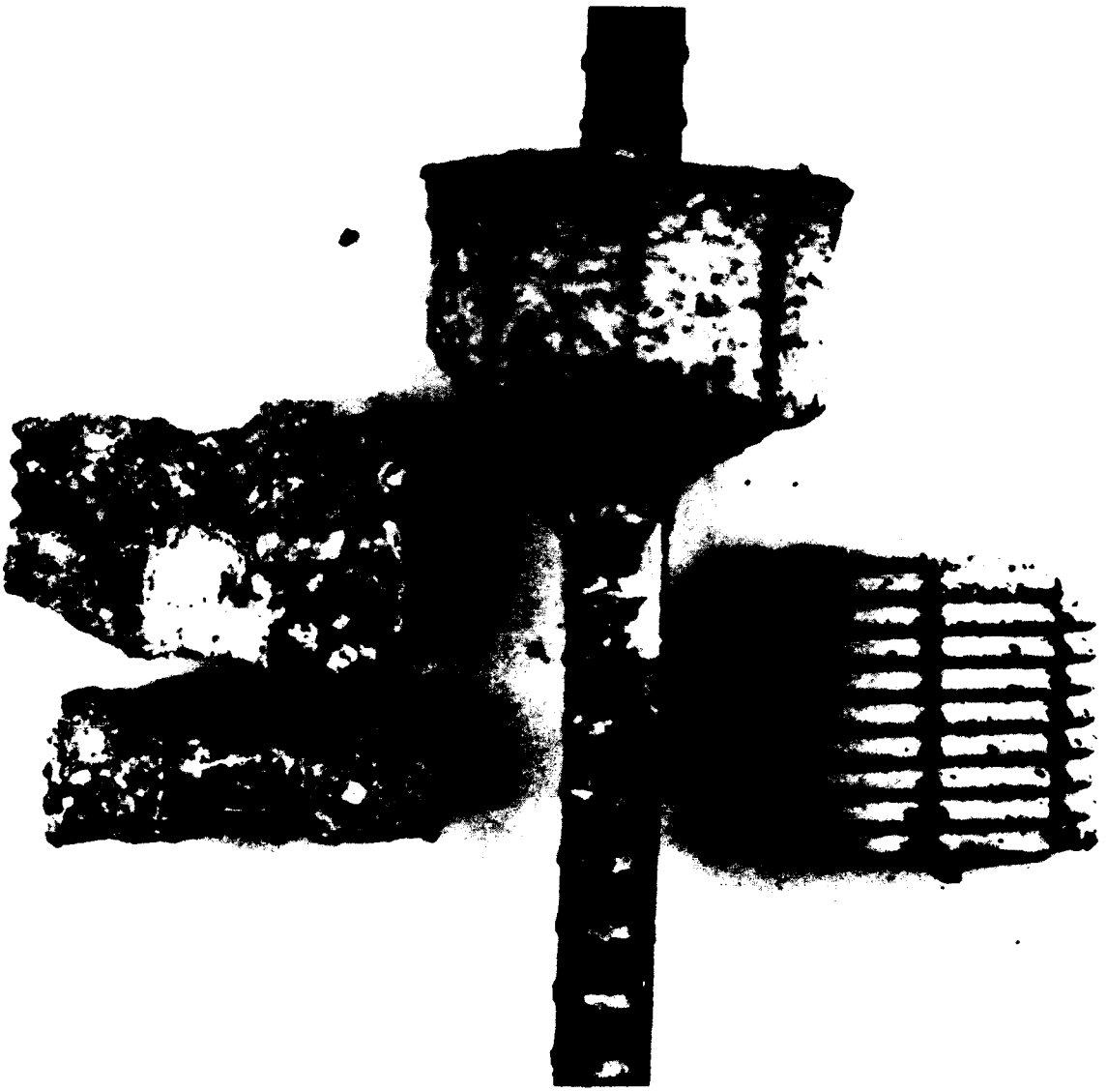

Figure 17.
View of Specimen 7 after failure.

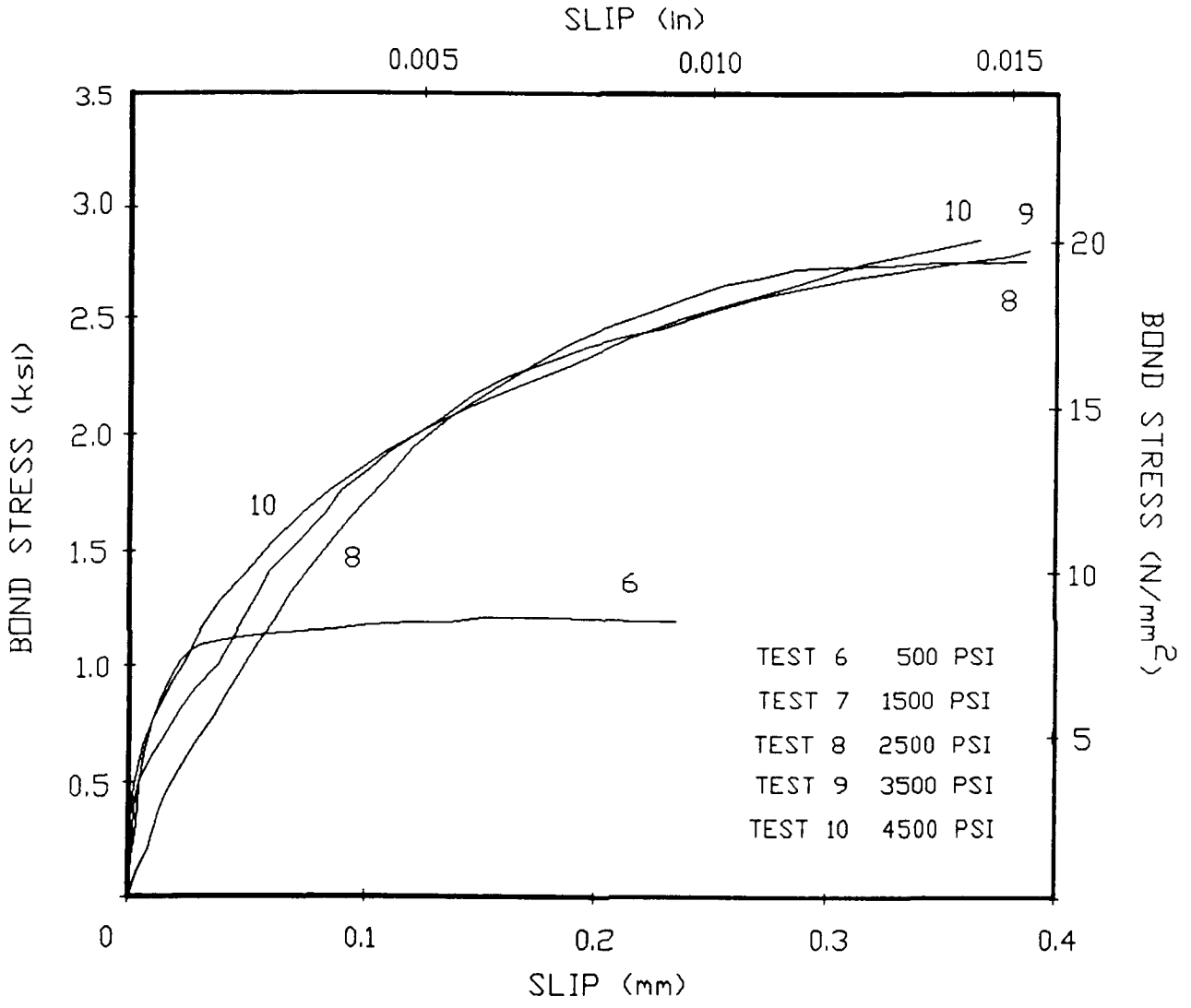


Figure 18.
Tests 6 through 10: Initial post-cracking bond-slip.

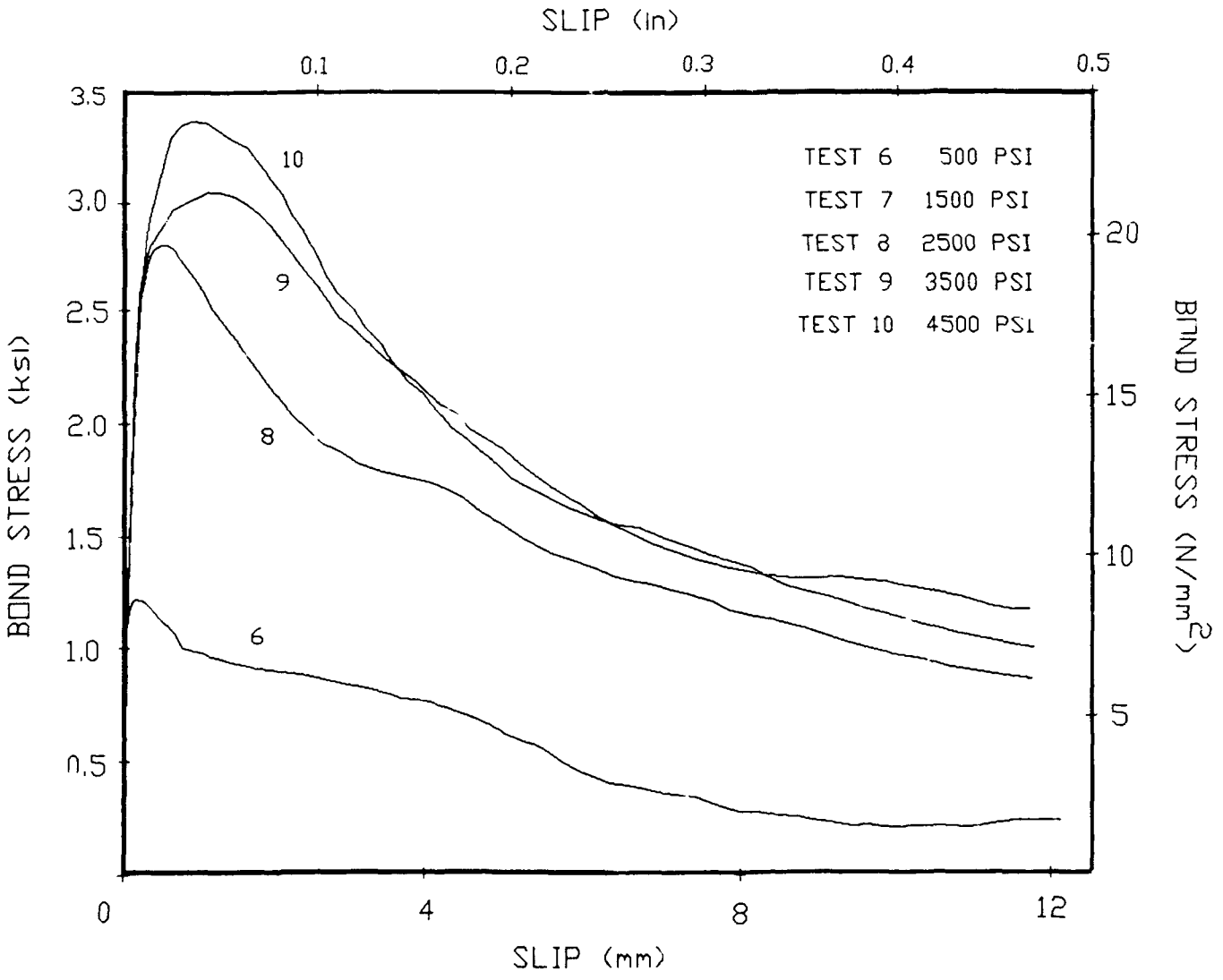


Figure 19.
Tests 6 through 10: Post-cracking bond-slip relationships.

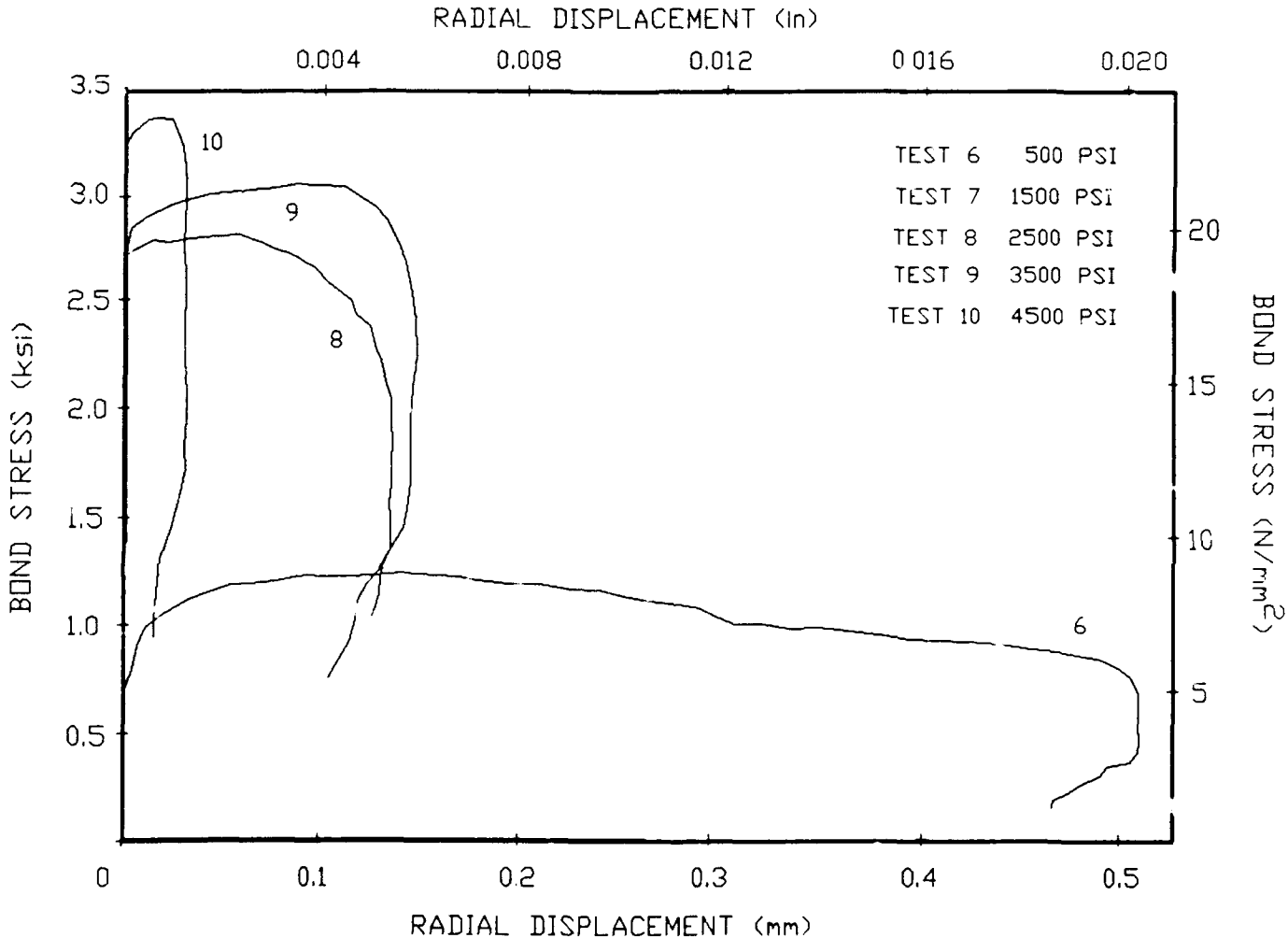


Figure 20.
Tests 6 through 10: Radial displacement histories.

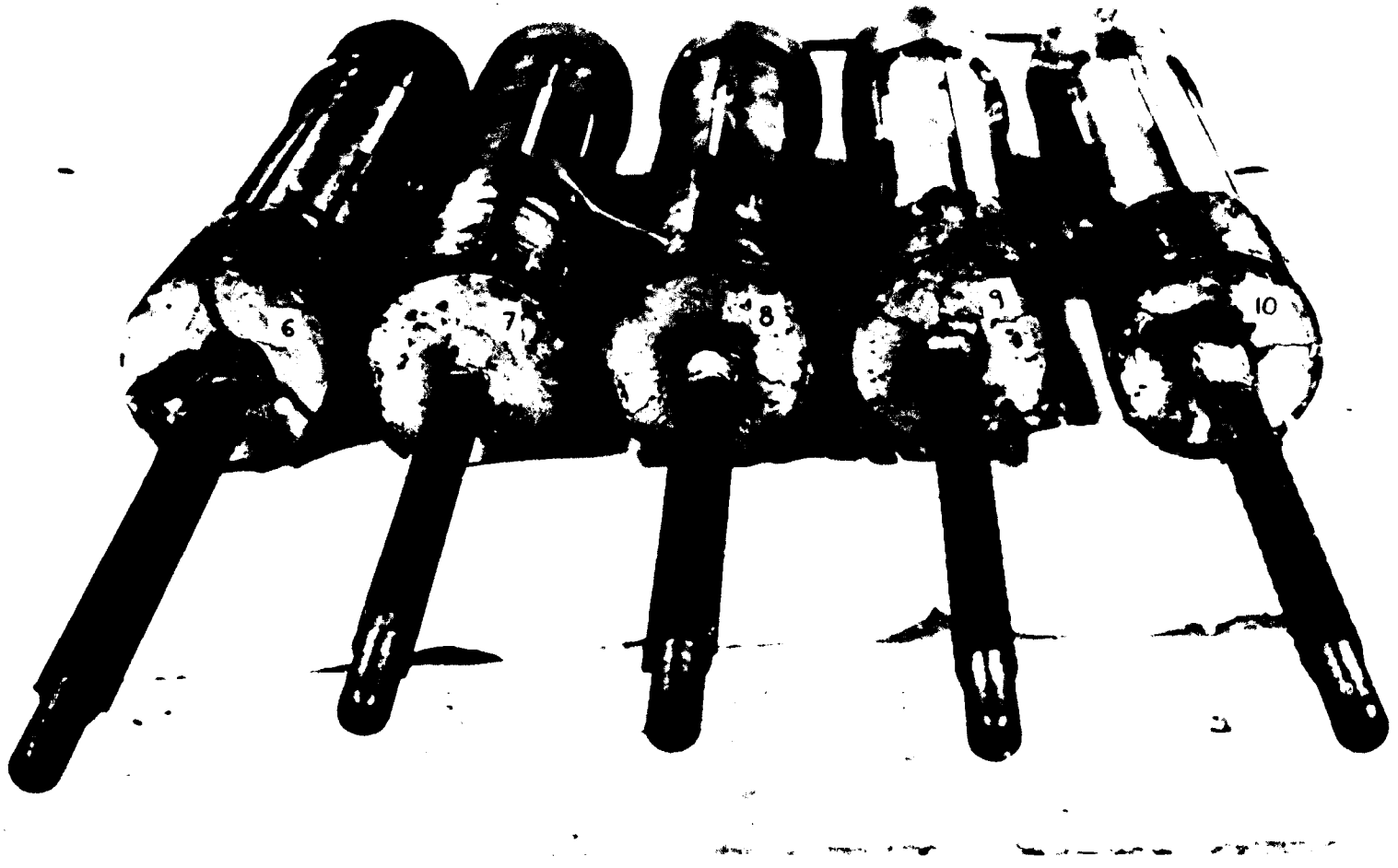


Figur[illegible]
Crack patterns in Tests 6 through 10.

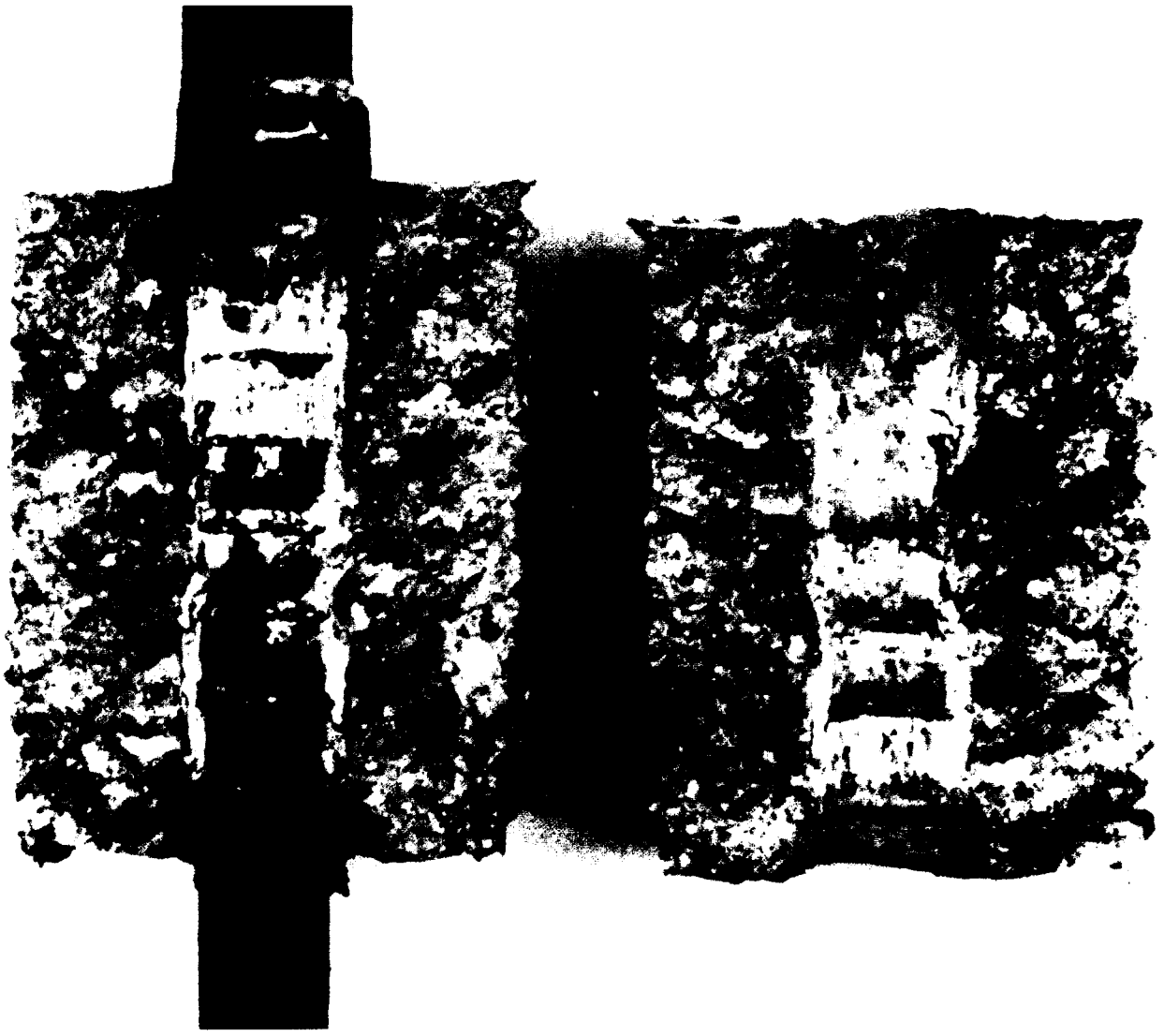

Figure 22.
View of Specimen 9 after failure.

**DISTRIBUTION LIST**

ARMY / R&D LAB, STRNC-UE, NATICK, MA
ARMY BELVOIR R&D CEN / STRBE-AALO, FORT BELVOIR, VA; STRBE-JB, FORT BELVOIR, VA
ARMY EWES / CEWES-CD-P, VICKSBURG, MS; WES-SS (KIGER), VICKSBURG, MS; WESGP-EM (CJ SMITH), VICKSBURG, MS
BETHLEHEM STEEL CO / ENGRG DEPT, BETHLEHEM, PA
CAL STATE UNIV / C.V. CHELAPATI, LONG BEACH, CA
CASE WESTERN RESERVE UNIV / CE DEPT (PERDIKARIS), CLEVELAND, OH
CINCUSNAVEUR / LONDON, UK, FPO NEW YORK
CLIFTON, B. / SPRINGFIELD, VA
COLLEGE OF ENGINEERING / CE DEPT (AKINMUSURU), SOUTHFIELD, MI; CE DEPT (GRACE), SOUTHFIELD, MI
CONRAD ASSOC / LUISONI, VAN NUYS, CA
COX, JIM / DAVIS, CA
DAMES & MOORE / LIB, LOS ANGELES, CA
GEORGE WASHINGTON UNIV / ENGRG & APP SCI SCHL (FOX), WASHINGTON, DC
GEORGIA INST OF TECH / CE SCHL (KAHN), ATLANTA, GA; CE SCHL (SWANGER), ATLANTA, GA; CE SCHL (ZURUCK), ATLANTA, GA
GIORDANO, A.J. / SEWELL, NJ
HEUZE, F / ALAMO, CA
HJ DEGENKOLB ASSOC / W. MURDOUGH, SAN FRANCISCO, CA
JOHN HOPKINS UNIV / CE DEPT, JONES, BALTIMORE, MD
LAWRENCE LIVERMORE NATL LAB / FJ TOKARZ, LIVERMORE, CA
NATL ACADEMY OF ENGRY / ALEXANDRIA, VA
NAVFACENGCOM / CODE 04A4E, ALEXANDRIA, VA
NAVSWC / DET, WHITE OAK LAB, TECH LIB, SILVER SPRING, MD
NIEDORODA, AW / GAINESVILLE, FL
NORDA / CODE 440, NSTL, MS
PENNSYLVANIA STATE UNIV / GOTOLSKI, UNIVERSITY PARK, PA
PMB ENGRG / LUNDBERG, SAN FRANCISCO, CA
PORTLAND STATE UNIV / ENGRG DEPT (MIGLIORI), PORTLAND, OR
PURDUE UNIV / CE SCOL (ALTSCHAEFFL), WEST LAFAYETTE, IN; CE SCOL (CHEN), WEST LAFAYETTE, IN; CE SCOL (LEONARDS), WEST LAFAYETTE, IN
PURSER, PAUL E. PE / HUMBLE, TX
SAN DIEGO STATE UNIV / CE DEPT (KRISHNAMOORTHY), SAN DIEGO, CA
SARGENT & HERKES, INC / JP PIERCE, JR, NEW ORLEANS, LA
SOUTHWEST RSCH INST / MARCHAND, SAN ANTONIO, TX
TEXAS A&M UNIV / CE DEPT (NIEDZWECKI), COLLEGE STATION, TX; CE DEPT (SNOW), COLLEGE STATION, TX
TRW INC / CRAWFORD, REDONDO BEACH, CA
TRW SPACE AND TECHNOLOGY GROUP / CARPENTER, REDONDO BEACH, CA
TUDOR ENGRG CO / ELLEGOOD, PHOENIX, AZ
UNIV OF CALIF / HERRMANN, DAVIS, CA; CE DEPT (FENVES), BERKELEY, CA; NAVAL ARCHT DEPT, BERKELEY, CA
UNIV OF HAWAII / CE DEPT (CHIU), HONOLULU, HI; RIGGS, HONOLULU, HI
UNIV OF MARYLAND / CE DEPT, COLLEGE PARK, MD
UNIV OF MICHIGAN / CE DEPT (RICHART), ANN ARBOR, MI
UNIV OF NEW MEXICO / NMERI (BEAN), ALBUQUERQUE, NM; NMERI (TAPSCOTT), ALBUQUERQUE, NM
UNIV OF PURDUE / DR J DAVID FROST, WEST LAFAYETTE, IN
UNIV OF RHODE ISLAND / CE DEPT (KOVACS), KINGSTON, RI; CE DEPT, KINGSTON, RI
UNIV OF WASHINGTON / CE DEPT (HARTZ), SEATTLE, WA

ADINA ENGRG, INC / WALCZAK, WATERTOWN, MA
APPLIED RSCH ASSOC, INC / HIGGINS, ALBUQUERQUE, NM
ARMY CORPS OF ENGRS / HQ, DAEN-ECE-D (PAAVOLA), WASHINGTON, DC
ARMY EWES / WES (NORMAN), VICKSBURG, MS; WES (PETERS), VICKSBURG, MS
CATHOLIC UNIV / CE DEPT (KIM), WASHINGTON, DC
CENTRIC ENGINEERING SYSTEMS INC / TAYLOR, PALO ALTO, CA
DOT / TRANSP SYS CEN (TONG), CAMBRIDGE, MA
HQ AFESC / RDC (DR. M. KATONA), TYNDALL AFB, FL
LOCKHEED / RSCH LAB (M. JACOBY), PALO ALTO, CA; RSCH LAB (P UNDERWOOD), PALO ALTO, CA
MARC ANALYSIS RSCH CORP / HSU, PALO ALTO, CA
MEDWADOWSKI, S. J. / CONSULT STRUCT ENGR, SAN FRANCISCO, CA
NAVFACENGCOM / CODE 04B2 (J. CECILIO), ALEXANDRIA, VA; CODE 04BE (WU), ALEXANDRIA, VA
NORTHWESTERN UNIV / BAZANT, EVANSTON, IL; CE DEPT (BELYTSCHKO), EVANSTON, IL
NRL / CODE 4430, WASHINGTON, DC
NSF / STRUC & BLDG SYSTEMS (KP CHANG), WASHINGTON, DC
OCNR / CODE 10P4 (KOSTOFF), ARLINGTON, VA
OREGON STATE UNIV / CE DEPT (LEONARD), CORVALLIS, OR
SCOPUS TECHNOLOGY INC / (B NOUR-OMID), EMERYVILLE, CA; (S NOUR-OMID), EMERYVILLE, CA
SRI INTL / ENGRG MECH DEPT (GRANT), MENLO PARK, CA; ENGRG MECH DEPT (SIMONS), MENLO PARK, CA
STANFORD UNIV / APP MECH DIV (HUGHES), STANFORD, CA; CE DEPT (PENSKY), STANFORD, CA; DIV OF APP MECH (SIMO), STANFORD, CA
TRW INC / CRAWFORD, REDONDO BEACH, CA
TUFTS UNIV / SANAYEI, MEDFORD, MA
UNIV OF CALIF / CE DEPT (HERRMANN), DAVIS, CA; CE DEPT (KUTTER), DAVIS, CA; CE DEPT (RAMEY), DAVIS, CA; CE DEPT (ROMSTAD), DAVIS, CA; CE DEPT (WILSON), BERKELEY, CA; CTR FOR GEOTECH MODEL (IDRISS), DAVIS, CA; FOURNEY, LOS ANGELES, CA; MECH ENGRG DEPT (BAYO), SANTA BARBARA, CA; MECH ENGRG DEPT (LECKIE), SANTA BARBARA, CA; MECH ENGRG DEPT (MCMEEKING), SANTA BARBARA, CA; SELMA, LOS ANGELES, CA
UNIV OF COLORADO / CE DEPT (HON-YIM KO), BOULDER, CO
UNIV OF ILLINOIS / CE LAB (ABRAMS), URBANA, IL; CE LAB (PECKNOLD), URBANA, IL
UNIV OF N CAROLINA / CE DEPT (GUPTA), RALEIGH, NC; CE DEPT (TUNG), RALEIGH, NC
UNIV OF WYOMING / CIVIL ENGRG DEPT, LARAMIE, WY

# NCEL DOCUMENT EVALUATION

You are number one with us; how do we rate with you?

We at NCEL want to provide you our customer the best possible reports but we need your help. Therefore, I ask you to please take the time from your busy schedule to fill out this questionnaire. Your response will assist us in providing the best reports possible for our users. I wish to thank you in advance for your assistance. I assure you that the information you provide will help us to be more responsive to your future needs.

R. N. STORER, Ph.D, P.E.
Technical Director

---

DOCUMENT NO. _____ TITLE OF DOCUMENT: _____

_____

---

Date: _____ Respondent Organization : _____

Name: _____ Activity Code: _____
Phone: _____ Grade/Rank: _____

Category (*please check*):

Sponsor ____ User ____ Proponent ____ Other (*Specify*) _____

Please answer on your behalf only; not on your organization's. Please check (*use an X*) only the block that most closely describes your attitude or feeling toward that statement:

**SA** Strongly Agree **A** Agree **O** Neutral **D** Disagree **SD** Strongly Disagree

---

| | | SA | A | N | D | SD |
|---|---|---|---|---|---|---|
| 1. | The technical quality of the report is comparable to most of my other sources of technical information. | ( ) | ( ) | ( ) | ( ) | ( ) |
| 2. | The report will make significant improvements in the cost and or performance of my operation. | ( ) | ( ) | ( ) | ( ) | ( ) |
| 3. | The report acknowledges related work accomplished by others. | ( ) | ( ) | ( ) | ( ) | ( ) |
| 4. | The report is well formatted. | ( ) | ( ) | ( ) | ( ) | ( ) |
| 5. | The report is clearly written. | ( ) | ( ) | ( ) | ( ) | ( ) |
| 6. | The conclusions and recommendations are clear and directly supported by the contents of the report. | ( ) | ( ) | ( ) | ( ) | ( ) |
| 7. | The graphics, tables, and photographs are well done. | ( ) | ( ) | ( ) | ( ) | ( ) |

Do you wish to continue getting NCEL reports? ☐ YES ☐ NO

Please add any comments (e.g., in what ways can we improve the quality of our reports?) on the back of this form.

**Comments:**

*Please fold on line and staple*

---

**DEPARTMENT OF THE NAVY**

Naval Civil Engineering Laboratory
Port Hueneme, CA 93043-5003

Official Business
Penalty for Private Use $300

Code L03B
NAVAL CIVIL ENGINEERING LABORATORY
PORT HUENEME, CA 93043-5003

## DISTRIBUTION QUESTIONNAIRE

**The Naval Civil Engineering Laboratory is revising its primary distribution lists.**

### SUBJECT CATEGORIES

**1 SHORE FACILITIES**
1A Construction methods and materials (including corrosion control, coatings)
1B Waterfront structures (maintenance/deterioration control)
1C Utilities (including power conditioning)
1D Explosives safety
1E Aviation Engineering Test Facilities
1F Fire prevention and control
1G Antenna technology
1H Structural analysis and design (including numerical and computer techniques)
1J Protective construction (including hardened shelters, shock and vibration studies)
1K Soil/rock mechanics
1L Airfields and pavements
1M Physical security

**2 ADVANCED BASE AND AMPHIBIOUS FACILITIES**
2A Base facilities (including shelters, power generation, water supplies)
2B Expedient roads/airfields/bridges
2C Over-the-beach operations (including breakwaters, wave forces)
2D POL storage, transfer, and distribution
2E Polar engineering

**3 ENERGY/POWER GENERATION**
3A Thermal conservation (thermal engineering of buildings, HVAC systems, energy loss measurement, power generation)
3B Controls and electrical conservation (electrical systems, energy monitoring and control systems)
3C Fuel flexibility (liquid fuels, coal utilization, energy from solid waste)
3D Alternate energy source (geothermal power, photovoltaic power systems, solar systems, wind systems, energy storage systems)
3E Site data and systems integration (energy resource data, integrating energy systems)
3F EMCS design

**4 ENVIRONMENTAL PROTECTION**
4A Solid waste management
4B Hazardous/toxic materials management
4C Waterwaste management and sanitary engineering
4D Oil pollution removal and recovery
4E Air pollution
4F Noise abatement

**5 OCEAN ENGINEERING**
5A Seafloor soils and foundations
5B Seafloor construction systems and operations (including diver and manipulator tools)
5C Undersea structures and materials
5D Anchors and moorings
5E Undersea power systems, electromechanical cables, and connectors
5F Pressure vessel facilities
5G Physical environment (including site surveying)
5H Ocean-based concrete structures
5J Hyperbaric chambers
5K Undersea cable dynamics

**ARMY FEAP**
BDG Shore Facilities
NRG Energy
ENV Environmental/Natural Responses
MGT Management
PRR Pavements/Railroads

### TYPES OF DOCUMENTS

**D** = Techdata Sheets; **R** = Technical Reports and Technical Notes; **G** = NCEL Guides and Abstracts; **I** = Index to TDS; **U** = User Guides; ☐ None - remove my name

## INSTRUCTIONS

The Naval Civil Engineering Laboratory has revised its primary distribution lists. To help us verify our records and update our data base, please do the following:

- Add - circle number on list
- Remove my name from all your lists - check box on list.
- Change my address - line out incorrect line and write in correction **(DO NOT REMOVE LABEL).**
- Number of copies should be entered after the title of the subject categories you select.
- Are we sending you the correct type of document? If not, circle the type(s) of document(s) you want to receive listed on the back of this card.

Fold on line, staple, and drop in mail.

**DEPARTMENT OF THE NAVY**

Naval Civil Engineering Laboratory
Port Hueneme, CA 93043-5003

Official Business
Penalty for Private Use, $300

**BUSINESS REPLY CARD**
FIRST CLASS PERMIT NO. 12503 WASH D.C.

POSTAGE WILL BE PAID BY ADDRESSEE

NO POSTAGE NECESSARY IF MAILED IN THE UNITED STATES

**Commanding Officer**
**Code L34**
**Naval Civil Engineering Laboratory**
**Port Hueneme, CA 93043-5003**